

Discovery of Potent and Fast-Acting Antimalarial Bis-1,2,4-triazines

Daniel L. Priebbenow, Mitch Mathiew, Da-Hua Shi, Jitendra R. Harjani, Julia G. Beveridge, Marina Chavchich, Michael D. Edstein, Sandra Duffy, Vicky M. Avery, Robert T. Jacobs, Stephen Brand, David M. Shackelford, Wen Wang, Longjin Zhong, Given Lee, Erin Tay, Helena Barker, Elly Crighton, Karen L. White, Susan A. Charman, Amanda De Paoli, Darren J. Creek, and Jonathan B. Baell*



Cite This: *J. Med. Chem.* 2021, 64, 4150–4162



Read Online

ACCESS |



Metrics & More

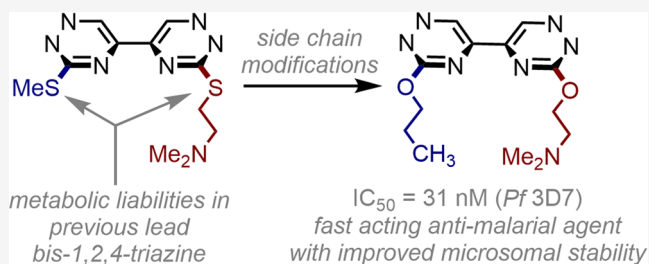


Article Recommendations



Supporting Information

ABSTRACT: Novel 3,3'-disubstituted-5,5'-bi(1,2,4-triazine) compounds with potent *in vitro* activity against *Plasmodium falciparum* parasites were recently discovered. To improve the pharmacokinetic properties of the triazine derivatives, a new structure–activity relationship (SAR) investigation was initiated with a focus on enhancing the metabolic stability of lead compounds. These efforts led to the identification of second-generation highly potent antimalarial bis-triazines, exemplified by triazine 23, which exhibited significantly improved *in vitro* metabolic stability (8 and 42 $\mu\text{L}/\text{min}/\text{mg}$ protein in human and mouse liver microsomes). The disubstituted triazine dimer 23 was also observed to suppress parasitemia in the Peters 4-day test with a mean ED_{50} value of 1.85 mg/kg/day and exhibited a fast-killing profile, revealing a new class of orally available antimalarial compounds of considerable interest.



INTRODUCTION

With over 200 million cases resulting in 409 000 deaths worldwide in 2019, malaria continues to have a significant negative impact on communities across Africa and South East Asia.¹ The human form of malaria is predominantly caused by the *Plasmodium falciparum* (*Pf*) parasite that infects red blood cells (RBCs) and when left untreated can lead to death.² Unfortunately, the emergence of *Pf* strains that are resistant to existing antimalarial therapeutics has exacerbated the impact of this devastating disease.³

The complexity of the malaria parasite lifecycle ensures that the discovery and development of new preventions and treatments remains a challenge.² This was exemplified in a recent review that highlighted the challenges associated with the discovery and development of four new small molecule antimalarial therapeutic agents (DSM26S,^{4–8} KAE609,^{9–11} KAF156,^{12,13} and MMV048^{14–17}).¹⁸

Despite exciting progress in the development of new therapeutic strategies, there remains an ongoing need to identify new antimalarial agents that act *via* a novel mode of action.¹⁸ To this end, we recently reported the discovery of 3,3'-disubstituted-5,5'-bi(1,2,4-triazine) (1), active against *Pf* with single-digit nanomolar activity and several thousand-fold lower toxicity to mammalian cells, demonstrating excellent selectivity (Figure 1).¹⁹

Triazine 1 exhibited equipotent activity against chloroquine and artemisinin-resistant laboratory strains of *Pf* and field isolates of *Pf* and *Plasmodium vivax*. Subsequent pharmacoki-

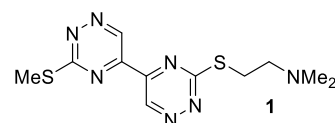


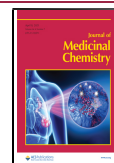
Figure 1. 1,2,4-bis-triazine identified as highly active against *Pf* in previous studies.

netic (PK) studies revealed rapid clearance and low exposure of the parent compound *in vivo*, but excellent *in vivo* activity was observed in the 4-day Peter's test in the *Plasmodium berghei* murine malaria model.²⁰ The mechanism of action of triazine 1 remains unknown; however, the unique structure when compared with known antimalarial agents, as well as equipotency against several resistant strains, suggests that compounds of this type act at a novel biological target.

Previous investigations into this class of compounds revealed that triazine 1 led to a rapid onset of action against all asexual blood stages, resulting in the sustained suppression of parasitaemia *in vivo* and demonstrated the inability to easily select for resistance, which implied a fast-killing profile, all

Received: January 11, 2021

Published: March 24, 2021

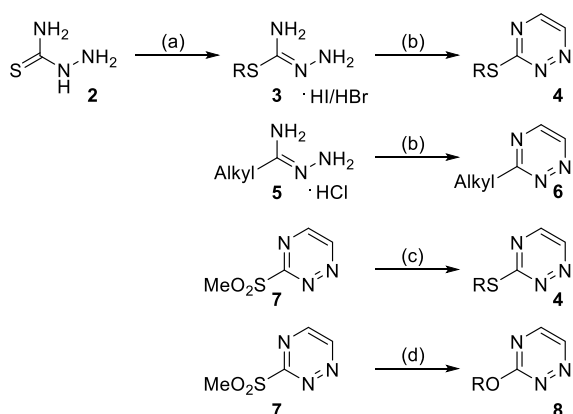


highly attractive properties of antimalarial small molecule therapeutics. To enable further development of these compounds for the treatment of uncomplicated malaria, this project involved a new structure–activity relationship (SAR) study to interrogate the pharmacokinetic liabilities associated with triazine **1**, in particular the basis for rapid clearance.

RESULTS AND DISCUSSION

Chemistry. The monomers were synthesized as outlined in **Scheme 1** using well-established methods.^{19,21,22} Predom-

Scheme 1. Synthesis of Triazine Monomers^a



^aReagents and conditions: (a) RBr/NaI or RI, EtOH, 81 °C; (b) 40% aq glyoxal, NaHCO₃, 0 °C then room temperature (rt); (c) RSH/Na₂CO₃, MeCN, rt; (d) NaH/ROH or MeMgI/ROH, *N,N*-dimethylformamide (DMF), rt.

inantly, 3-(alkylthio)-1,2,4-triazines **4** were accessed from *S*-alkyl thiosemicarbazides **3** by employing a condensation reaction with aqueous (aq) glyoxal. A condensation process was also employed to access 3-alkyl-1,2,4-triazines **6** from the corresponding hydrazonamides **5**. Alternatively, 3-(alkylthio)-1,2,4-triazines **4** could be prepared *via* the nucleophilic substitution of 3-(methylsulfonyl)-1,2,4-triazines **7** with mercaptans and 3-(alkoxy)-1,2,4-triazines **8** were prepared using a similar strategy employing alkoxy nucleophiles derived from alcohols.

To access the 3,3'-disubstituted-5,5'-bi(1,2,4-triazine) derivatives, a cyanide-mediated dimerization process was employed using equimolar mixtures of the requisite monomers (**Scheme 2**). The use of structurally different monomers typically afforded a product mixture comprising both the heterodimer and the two possible homodimers (**Scheme 2**), each of which was readily separated and subsequently subjected to biochemical evaluation.

The overarching aim of this investigation was to gain additional insight into the SAR of the triazine to discover new compounds that were highly potent against *Pf*, yet possessed

improved pharmacokinetic properties. For the active compounds previously identified (e.g., **1**), multiple sites were identified at which metabolic oxidation could occur, including (i) the sulfur atom within the thioether motif; (ii) one of the multiple heteroaryl nitrogen atoms; or (iii) the nitrogen within the tethered amine group. To explore this further, initial investigations focused on retaining the right hand side (RHS) thioethylamine tether, and either (i) increasing the bulk around the left hand side (LHS)-SMe motif to retard oxidation at this site or (ii) replacing the thioether with a functional group less susceptible to metabolic oxidation (**Table 1**).

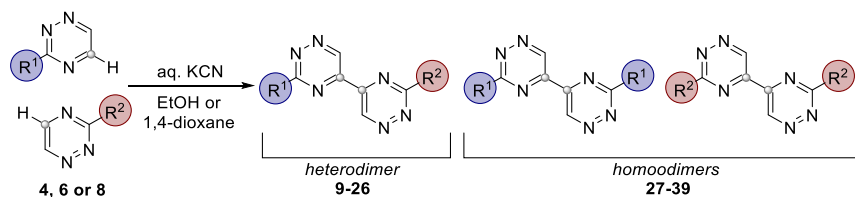
Table 1. SAR Exploring LHS Substitution within Thioether-Derived 3,3'-Disubstituted-5,5'-Bi(1,2,4-triazine)s against *In Vitro Pf* 3D7 Proliferation

compound	R ¹	3D7 IC ₅₀ (μM) ^a
1	-SMe	0.0080
9	-S ⁱ Pr	0.21
10	-S(CH ₂) ₂ OMe	0.26
11	-OMe	0.85
12	-O ⁿ Pr	0.011
13	-O ⁱ Pr	0.081
14	-O ^o Pr	0.013
15	-Et	0.12 ± 0.085
16	- ⁿ Bu	0.0090 ± 0.0004

^aValues represent outcomes from one or two experiments (for two experiments, the values represent the mean, with “±” sign representing the standard deviation (S.D.)) against *Pf* 3D7 strain, erythrocyte stage (chloroquine control, half-maximal inhibitory concentration (IC₅₀) = 0.004 μM).²³

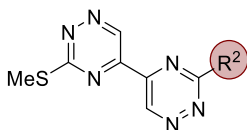
Using triazine **1** as a template, initial efforts to increase the bulk of the thioether group to mitigate metabolism (if occurring at this site) involved the synthesis of the isopropyl (**9**, IC₅₀ = 0.21 μM) and ethyl methyl ether (**10**, IC₅₀ = 0.26 μM) derivatives; however, both substitution patterns led to a significant decrease in antimalarial activity. *O*-Alkyl substitution at this position was then explored to mitigate the oxidation of the thioether functionality, with the methoxy analogue (**11**, IC₅₀ = 0.85 μM) exhibiting relatively poorer antimalarial activity when compared with the *n*-propoxy **12**, isopropoxy **13**, and cyclopropoxy **14** derivatives, which all showed very potent IC₅₀ values of 0.011, 0.081, and 0.013 μM, respectively, against the *Pf* 3D7 strain. Two additional examples containing no heteroatoms within the LHS tether were then prepared with the butyl analogue **16**, exhibiting 13-fold greater antimalarial activity (IC₅₀ = 9.0 nM) than the corresponding ethyl derivative (**15**, IC₅₀ = 0.12 μM).

Scheme 2. Cyanide-Mediated Dimerization Protocol was Employed to Prepare Both Hetero- and Homodimeric Triazines



As the RHS thioethylamino chain ($-\text{S}(\text{CH}_2)_2\text{NMe}_2$) present in **1** was also previously identified as a possible site of oxidation leading to poor metabolic stability, subsequent efforts focused on retaining the SMe on LHS and varying the RHS chain to remove the sulfur, amine, or both (Table 2).

Table 2. SAR Exploring RHS Substitution within Thioether-Derived 3,3'-Disubstituted-5,5'-Bi(1,2,4-triazine)s against *In Vitro* Pf 3D7 Proliferation



compound	R ²	3D7 IC ₅₀ (μM) ^a
17	$-\text{S}-\text{CH}_2\text{C}\equiv\text{CH}$	0.032 ± 0.017
18	$-\text{S}(\text{CH}_2)_3\text{N}_3$	0.0044 ± 0.0002
19	$-\text{O}(\text{CH}_2)_2\text{NMe}_2$	0.080
20	$-\text{OCH}(\text{Me})\text{CH}_2\text{NMe}_2$	0.032 ± 0.083
21	$-\text{O}-\text{CH}_2\text{C}\equiv\text{CH}$	0.13 ± 0.030

^aValues represent outcomes from one or two experiments (for two experiments, the values represent the mean, with “±” sign representing the standard deviation) against *Pf* 3D7 strain, erythrocyte stage (chloroquine control, IC₅₀ = 0.004 μM).²³

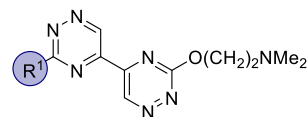
Substitution of the amino group with a propargyl group (**17**, IC₅₀ = 0.032 μM) led to a relatively active compound. The activity was also retained when the sulfur atom was replaced with an oxygen atom while keeping the tertiary amine tether (**19**, IC₅₀ = 0.080 μM and **20**, IC₅₀ = 0.032 μM). However, when both the sulfur and amine components were modified (**21**, IC₅₀ = 0.13 μM), a 20-fold loss of potency was observed in comparison to **1**. Intriguingly, the replacement of the ethylamino functionality with the propylazide afforded the most potent triazine dimer **18**, which exhibited exceptional antimalarial activity against *Pf* 3D7, exhibiting an IC₅₀ value of 4.4 nM.

Having shown that compound **19** (the oxygen analogue of **1**) was relatively active against the 3D7 line, this compound was used as the template for the next part of the investigation (Table 3). In a manner similar to that outlined above, the RHS oxyethylamine tether was kept constant and variations on the LHS tether were explored.

Whereas increased bulk on the LHS thioether in the previous series (Table 1) led to a loss of activity, for the oxyethylamino derivatives changing from the methyl thioether (**19**, IC₅₀ = 0.080 μM) to the isopropyl thioether **22** on the LHS increased activity with **22** exhibiting an excellent IC₅₀ value of 0.012 μM against the *Pf* 3D7 cell line. The analogous isopropoxy derivative (**24**, IC₅₀ = 0.44 μM) was relatively inactive; however, the *n*-propoxy compound **23** exhibited good activity with an IC₅₀ value of 0.031 μM. Removing the heteroatom from this chain was also tolerated in the form of the *n*-butyl derivative **26**, which exhibited excellent activity at 0.030 μM. The trifluoromethyl derivative **25** possessing the same chain length as *n*-propoxy analogue **23** also exhibited good antimalarial activity (IC₅₀ = 0.054 μM).

A consequence of the synthetic strategy employed to access the heterodimers discussed above (and those we have previously reported¹⁹) was the formation of homodimers of each monomer in the reaction system (refer to Scheme 2). As such, across our research program, we accumulated a series of

Table 3. SAR Exploring LHS Substitution within Ether-Derived 3,3'-Disubstituted-5,5'-Bi(1,2,4-triazine)s against *In Vitro* Pf 3D7 Proliferation

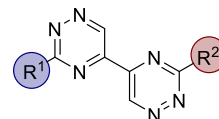


compound	R ¹	3D7 IC ₅₀ (μM) ^a
19	$-\text{SMe}$	0.080
22	$-\text{S}^i\text{Pr}$	0.012
23	$-\text{O}^n\text{Pr}$	0.031 ± 0.008
24	$-\text{O}^i\text{Pr}$	0.44 ± 0.029
25	$-\text{O}(\text{CH}_2)_2\text{CF}_3$	0.054 ± 0.001
26	$-\text{nBu}$	0.030 ± 0.008

^aValues represent outcomes from one or two experiments (for two experiments, the values represent the mean, with “±” sign representing the standard deviation) against *Pf* 3D7 strain, erythrocyte stage (chloroquine control, IC₅₀ = 0.004 μM).²³

homodimeric analogues. To gain additional insight into SAR, as a part of this study, these homodimers were screened for activity with the results outlined in Table 4.

Table 4. SAR Exploring Homodimeric 3,3'-Disubstituted-5,5'-Bi(1,2,4-triazine)s against *In Vitro* Pf 3D7 Proliferation



compound ID	R ¹ = R ²	3D7 IC ₅₀ (μM) ^a
27	$-\text{S}(\text{CH}_2)_3\text{N}_3$	0.031 ± 0.002
28	$-\text{nBu}$	0.34 ± 0.043
29	$-\text{O}^n\text{Pr}$	0.11 ± 0.014
30	$-\text{O}^i\text{Pr}$	2.0
31	$-\text{O}^o\text{Pr}$	0.89
32	$-\text{O}(\text{CH}_2)_2\text{CF}_3$	0.093 ± 0.006
33	$-\text{O}(\text{CH}_2)_2\text{SiMe}_3$	0.72 ± 0.033
34	$-\text{OCH}_2\text{CF}_3$	0.42 ± 0.115
35	$-\text{O}(\text{CH}_2)_2\text{OMe}$	100% @ 40 μM
36	$-\text{O}-\text{CH}_2\text{CH}_2(4\text{-methylthiazol-5-yl})$	0.50 ± 0.123
37	$-\text{O}-(\text{CH}_2)_2\text{NMe}_2$	8.6 ± 0.339
38	$-\text{O}-\text{CH}(\text{Me})\text{CH}_2\text{NMe}_2$	12 ± 1.13
39	$-\text{O}-\text{CH}_2\text{C}\equiv\text{CH}$	1.0 ± 0.111

^aValues represent outcomes from one or two experiments (for two experiments, the values represent the mean, with “±” sign representing the standard deviation) against *Pf* 3D7 strain, erythrocyte stage (chloroquine control, IC₅₀ = 0.004 μM).²³

We had previously observed that the symmetrical homodimers containing thioether tethers were relatively active (up to IC₅₀ = 0.017 μM),¹⁹ whereas the bis(methoxy) triazine dimer was inactive. For the series evaluated during this study, it was observed that the thioethylazide dimer (**27**) was as potent as some of the heterodimers, exhibiting an IC₅₀ value of 0.031 μM. The *n*-propoxy (**29**) and corresponding trifluoromethyl analogue (**32**) were also active against the *Pf* 3D7 cell line (IC₅₀ values of 0.11 and 0.093 μM, respectively); however, the remainder of oxo-tethered homodimeric analogues screened were all relatively inactive exhibiting values between 0.34 and 12 μM (Table 4, entries 4, 7–13).

Table 5. Physicochemical Parameters and *In Vitro* Metabolism in Liver Microsomes of Selected Triazine Derivatives

compd	MW	PSA (Å ²) ^a	partition coefficient	solubility (μg/mL) ^b		<i>in vitro</i> CL _{int} ^c (μL/min/mg protein) [h/m]	<i>in vitro</i> degradation half-life (min) [h/m]
			(clog P)	pH 2.0	pH 6.5		
1	309.41	82	1.0	6.3–12.5	6.3–12.5	15/138	113/13
15	291.38	82	0.4	50–100	25–50	9/118	199/15
16	319.43	82	1.3	50–100	25–50	56/330	31/5
23	305.34	100	0.5	>100	>100	8/42	229/42
25	359.31	100	0.1	50–100	50–100	7/33	232/53
26	303.36	91	0.7	25–50	25–50	25/109	69/16

^aCalculated using Chem Axon JChem software. ^bKinetic solubility determined by nephelometry. ^c*In vitro* intrinsic clearance (CL_{int}) determined in human (h) or mouse (m) liver microsomes (HLM or MLM).

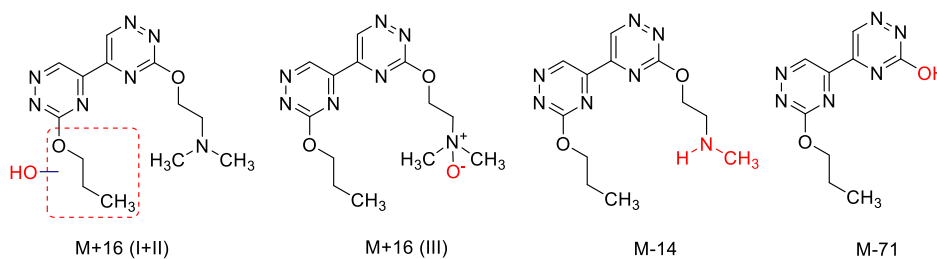


Figure 2. Major metabolites (based on peak area) detected in incubations with hepatic microsomes and cryopreserved hepatocytes. Metabolite M +16 (III) appeared to be the main metabolite in both test systems based on the peak area. The dashed lines represent the region of the molecule where oxidation is thought to occur; however, the exact site could not be confirmed.

Physicochemical Parameters and Predictive Absorption, Distribution, Metabolism, and Excretion (ADME).

The overarching aim of this investigation was to address the relatively poor solubility and metabolic stability of the previously identified lead compound. Five new compounds with potent antimalarial activity against *Pf* were subjected to the preliminary evaluation of drug-likeness with the results compared to the previous lead compound 1 (Table 5).

As shown in Table 5, the molecular weight (MW) of each compound was well below 500 g/mol, the topological polar surface area (PSA) ranged from 82 to 100 Å², which is within a range that is likely to be conducive to good passive cellular permeability²⁴ and kinetic solubility in some cases was greater than 100 μg/mL. Overall, the compounds evaluated throughout this investigation demonstrated a much improved solubility when compared with 1, predisposing these triazine dimers favorably toward oral bioavailability.

To enable the further development of early leads, compounds are ideally not rapidly metabolized, which would improve the likelihood of good oral bioavailability and reasonable *in vivo* half-life ($T_{1/2}$). During this study, the metabolic stability of selected triazines was evaluated initially in human and mouse liver microsomes (referred to as HLM and MLM, respectively) at 37°C (Table 5, see the Supporting Information (SI) for methods). These data provide key insights into the structural features of the 3,3'-disubstituted triazine dimers that render such molecules less susceptible to rapid hepatic metabolism. Selected compounds were also evaluated using cryopreserved hepatocytes to determine the possibility of metabolism by routes that are not present in the microsomal fraction (see the SI for methods).

Replacing the LHS thioether (–SMe) with an alkyl group (–Et, triazine 15) resulted in an increase in microsomal stability (HLM CL_{int} = 9 μL/min/mg protein); however, this modification also resulted in a considerable drop in potency

(IC₅₀ = 0.12 μM). Extension of this alkyl chain to the *n*-butyl group restored potency (triazine 16, IC₅₀ = 0.009 μM); however, this analogue was rapidly metabolized in both HLM and MLM (Table 5). The ether version of this *n*-butyl analogue 26, which exhibited an IC₅₀ value of 0.030 μM against *Pf*, was also more rapidly metabolized in both HLM and MLM than triazine 1 (Table 5).

The best performing compounds identified from this evaluation were the bis-ether triazine derivatives 23 and 25 (Table 5), which demonstrated potent antimalarial activity with IC₅₀ values of 0.031 and 0.054 μM, respectively, against the *Pf* 3D7 strain. Inclusion of the terminal –CF₃ group (25) in place of the –CH₃ group (23) offered no apparent advantage, with triazine 23 exhibiting the best solubility and metabolic stability in both HLM (CL_{int} = 8 μL/min/mg protein) and MLM (CL_{int} = 42 μL/min/mg protein). The CL_{int} value was marginally higher in rat liver microsomes (66 μL/min/mg protein). These results represent a significant improvement in microsomal stability for these second-generation triazine dimers (in particular 23) with only a minor loss in potency when compared to the previous lead compound, triazine 1. The stability of 23 was also evaluated in human, rat, and mouse cryopreserved hepatocytes, where the *in vitro* CL_{int} values were 3.6, 10, and 3.7 μL/min/10⁶ cells, respectively.

Metabolite predictions were conducted using the software package Meteor Nexus (Lhasa Ltd., U.K.) and the predicted plausible primary metabolites included three +16 oxygenation metabolites (an amine oxide of a tertiary amine, hydroxylation of a terminal methyl, hydroxylation of penultimate alkyl methylene), oxidative N-demethylation, and oxidative O-dealkylation, amongst others. Metabolite identification studies with 23 were conducted using samples from incubations with hepatic microsomes (see the SI for methods) with structure confirmation supported by tandem mass spectrometry (MS/

MS) (collision-induced dissociation (CID)) spectral analysis where possible. Three prominent oxygenated metabolites (Figure 2, designated M+16 (I, II, and III)) were detected, with M+16 (I and II) mainly forming in HLM and M+16 (III) being the predominant metabolite across species based on the peak area (authentic standards not available). Based on CID spectra, M+16 (III) appears to be the *N*-oxide with M+16 (I and II) being the terminal and penultimate hydroxylation sites. Other metabolites included an *N*-demethylation product (Figure 2, M-14) and O-dealkylation of the ethyl dimethylamine tether (Figure 2, M-71); both primarily detected in RLM and MLM but not in HLM. A further cleavage product (M-69) was detected in all three species both in the absence and presence of reduced nicotinamide adenine dinucleotide phosphate (NADPH); however, the identity of this species has not yet been determined. The metabolite profile was similar when incubated with hepatocytes, with no conjugated metabolites (e.g., glucuronides or sulfates) detected.

Additional *in vitro* assays were conducted with **23** to determine rat plasma protein binding (PPB), the blood-to-plasma (B/P) partitioning ratio, blood and plasma stability, Caco-2 permeability, and cytochrome (CYP) inhibition. The results for these are summarized in Table 6 (see the SI for

Table 6. Predicted *In Vivo* Unbound Hepatic Intrinsic Clearance ($CL_{int,unb}$), Plasma Protein Binding (PPB), Blood-to-Plasma (B/P) Partitioning Ratio, Caco-2 Permeability (P_{app}), and CYP Inhibition for **23**^a

parameter	value
predicted <i>in vivo</i> $CL_{int,unb}$ (mL/min/kg)	
microsomes [h/r/m]	6.8/117/112
hepatocytes [h/r/m]	9.5/49/27
PPB (% bound) [r]	22
B/P [r]	1.3
P_{app} (10^{-6} cm/s)	
A - B	40
B - A	46
efflux ratio	1.1
CYP inhibition (IC_{50} , μ M)	
CYP1A2, 2C9, 2C19, 2D6, 3A4 (midazolam 1'-hydroxylation), 3A4 (testosterone 6 β -hydroxylation)	>20 for all isoforms

^aWhere noted, values correspond to the human [h], rat [r], or mouse [m] test systems.

methods). Plasma protein binding in rat plasma was low, B/P indicated effective distribution into erythrocytes, and permeability was high with no evidence of efflux. *Ex vivo* studies with **23** in rat and mouse blood indicated some instability, with 15 and 23% loss of parent, respectively, over a 4 h incubation. There was no evidence of significant inhibition of the 5 major CYP isoforms, suggesting a low likelihood of significant drug-drug interactions of coadministered compounds that are metabolized by these enzymes.

After scaling and correcting for compound binding, both hepatic microsomes and hepatocytes predicted that **23** would have a higher unbound hepatic intrinsic clearance ($CL_{int,unb}$) in rats and mice compared to humans (Table 6), although this species difference was more marked in hepatocytes. There was no evidence to suggest that **23** was subject to metabolism by enzymes that were not present in the microsomal test system (e.g., aldehyde oxidase, conjugative enzymes), as values for the predicted unbound intrinsic clearance in rats and mice were

higher in microsomes than in hepatocytes, albeit that transporter insufficiency in cryopreserved hepatocytes could mask the true extent of intact hepatocyte metabolism.

In Vitro Parasite Reduction Ratio (PRR). Antimalarials with a fast-killing profile are highly desirable as they reduce the likelihood of the parasite developing resistance. Triazine **23** was evaluated against the *P. falciparum* 3D7A laboratory line in the PRR model²⁵ (two-point FACS) at a concentration of ten times the IC_{50} value using artesunate, chloroquine, pyrimethamine, and atovaquone for comparison, where it demonstrated a fast-killing profile similar to that of both artesunate and chloroquine (Figure 3).

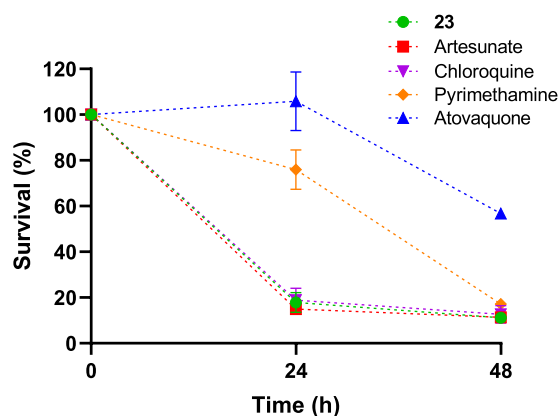


Figure 3. Percentage survival of *P. falciparum* 3D7A parasites after treatment with **23** and standard antimalarials. Data points represent the mean \pm standard deviation (S.D.) ($n = 3$ replicates).

Activity against Drug-Resistant Strains. When the antimalarial activity of **23** was assessed against a panel of laboratory strains with mutations in recently identified targets using a standard ³H-incorporation growth inhibition assay,²⁶ **23** was observed to be equipotent against all strains tested, again indicating that the antimalarial activity is instigated *via* a novel mechanism of action (Figure 4). The IC_{50} value for **23** obtained from this *in vitro* assay against NF54 was 0.021 μ M. Against the K1, 7G8, TM90C2B, RF12, MRA1240, and Dd2 lines, the IC_{50} value was determined to range from 0.023 to

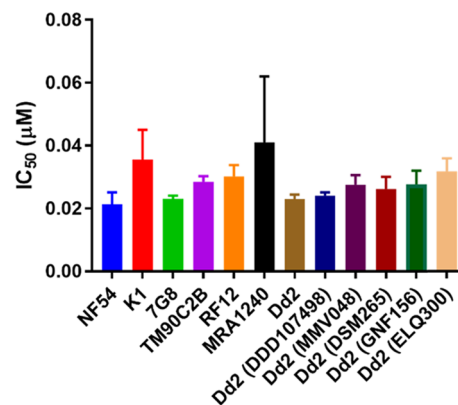


Figure 4. Antimalarial activity of triazine **23** against laboratory field strains and laboratory-generated resistant strains.^{8,17,26–29} Data represent the mean \pm range ($n = 2$ replicates). Compounds in parentheses were used to generate the resistant strains.

0.041 with a fold shift of 1.1–1.95 relative to its potency against NF54, which is indicative of a lack of cross-resistance.

Dual Gamete Formation Assay (DGFA). Gametocytes are quiescent in the human host and only undergo differentiation into the active sexual stages upon insect blood feeding and transfer into the mosquito midgut. The DGFA is a convenient assay, which is highly predictive of the transmission-blocking potential of compounds, and investigates the “functional viability” of mature stage V gametocytes undergoing onward differentiation into male and female gametes.³⁰ Intriguingly, early members of the triazine series previously demonstrated activity against early-stage gametocytes but not against mature gametocytes (stage V). In this study, triazine **23** was not particularly potent in the DGFA, compared to its blood stage activity, exhibiting EC₅₀ values of 1.2 and 2.9 μM for male and female gametocytes, respectively. This would suggest that at therapeutic (*i.e.*, TCP-1, treatment) concentrations, the compound would have negligible transmission-blocking potential. Compounds with good transmission potential are generally considered as those that have comparable potency in DGFA and blood stages, for example, KAE609 and KAF156.³¹

3-(4,5-Dimethylthiazol-2-yl)-2,5-diphenyltetrazolium Bromide (MTT) Assay to Assess Cytotoxicity. An MTT assay was then conducted to assess the cytotoxicity of **23** (see the SI for methods), which exhibited an EC₅₀ value of 36 μM, providing a “selectivity index” of >1000 (HEK CC50/3D7 IC₅₀) and suggesting a low likelihood of interaction of **23** with critical host cell metabolic processes.

Pharmacokinetic Properties. We then undertook mouse and rat pharmacokinetic studies for the most promising candidate, triazine **23** (see the SI for methods). As shown in Figure 5 and Table 7, intravenous (IV) dosing of **23** to mice at

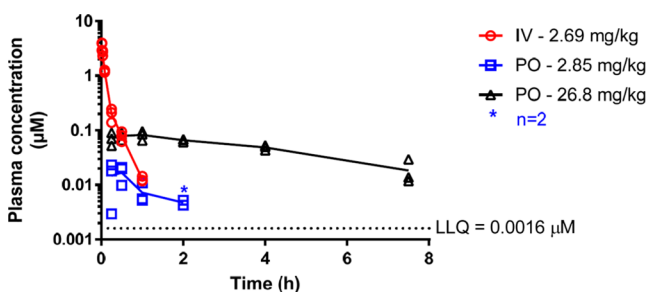


Figure 5. Plasma concentrations of **23** in male Swiss outbred mice following IV and oral administration.

2.7 mg/kg resulted in a rapid decline in plasma concentrations, which were below the limit of quantitation by 2 h such that the terminal phase was not well-defined (Figure 5). The estimated plasma clearance was very high (~400 mL/min/kg) and considerably above hepatic blood flow in the mouse, suggestive of extrahepatic clearance mechanisms. Given its very low calculated Log $D_{7,4}$ (−0.5), it was proposed that **23** might be renally eliminated; however, urine was not collected following dosing to mice.

Following oral administration at a low dose of 2.8 mg/kg, **23** was detected for 2 h after the dose was administered (Figure 5). After oral dosing at 27 mg/kg, **23** demonstrated plasma concentrations below ~30 mg/mL, an apparent half-life of ~3 h, and a measurable but low oral bioavailability of 12% (Figure 5).

Table 7. Pharmacokinetic Parameters for **23 in Male Swiss Outbred Mice Following IV and Oral Administration**

parameter	IV administration	PO administration	
		low dose	high dose
calculated dose (mg/kg)	2.69	2.85	26.8
apparent $t_{1/2}$ (h)	0.20 ^a	nd ^b	3.0
plasma C_{max} (μM)		0.0168	0.0820
T_{max} (h)		0.50	1.0
plasma AUC _{0-inf} (μM*h)	0.36 ^a	0.038 ^b	0.44
plasma CL (mL/min/kg)	406 ^a		
plasma V_{ss} (L/kg)	3.4 ^a		
BA (%)		10	12

^aValues are approximate only as plasma concentrations were only above the analytical limit of quantitation for 1 h postdose. ^bThe terminal phase for the low dose per os (PO) group was not well-defined; the terminal phase rate constant for the high dose PO group was used to estimate AUC_{0-inf}.

Building on these results, a pharmacokinetic study with **23** was then undertaken in Sprague Dawley rats with IV (3 mg/kg) and oral (10 mg/kg) administration (see the SI for methods). Plasma concentration *versus* time profiles are shown in Figure 6, and pharmacokinetic parameters are presented in Table 8.

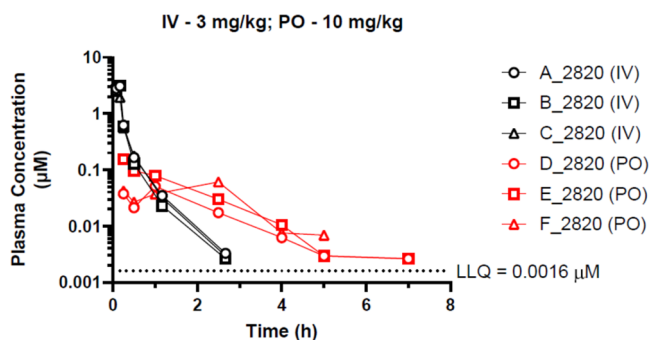


Figure 6. Plasma concentrations of **23** in male Sprague Dawley rats following IV and oral administration.

Similar to the data in mice, measurable plasma concentrations after IV dosing to rats were only observed up to 2.5 h. The estimated IV half-life was approximately 0.4 h and plasma CL and V_{ss} were both high. Given the blood-to-plasma ratio of

Table 8. Pharmacokinetic Parameters for **23 after IV (3 mg/kg) and Oral (10 mg/kg) Administration to Male Sprague Dawley Rats**

parameter	IV administration	PO administration
calculated dose (mg/kg)	3.0	10
apparent $t_{1/2}$ (h)	0.39 ^a	nd ^b
plasma C_{max} (μM)		0.0894
T_{max} (h)		1.3
plasma AUC _{0-inf} (μM*h)	0.658 ^a	nd
plasma CL (mL/min/kg)	249 ^a	
plasma V_{ss} (L/kg)	2.80 ^a	
BA (%)		7.49

^aValues are approximate only as plasma concentrations were only above the analytical limit of quantitation for 2.5 h postdose. ^bCould not calculate due to insufficient definition of the terminal elimination phase.

1.3, the apparent blood clearance (205 mL/min/kg) was substantially higher than the nominal hepatic blood flow in the rat (~67.6 mL/min/kg), which again suggested that 23 is subject to extrahepatic elimination. Renal elimination represented a relatively minor *in vivo* clearance pathway with less than 3% of the IV dose recovered unchanged in urine over 24 h postdose. Following oral administration to rats, maximum plasma concentrations were observed at 0.25–2.5 h. The apparent oral bioavailability (based on AUC_{0–last}) ranged from 5 to 10%.

Metabolite identification studies with selected plasma, urine, and feces samples from the rat PK study were further analyzed using high-resolution mass spectrometry (HRMS). Metabolite screening was limited to the previously detected metabolites (Figure 2) and selected phase II conjugation reactions (even though these were not detected *in vitro*). Three oxygenation products (M+16, Figure 2), a bis-oxygenation (M+32), and demethylation (M–14) products were detected in urine and fecal samples from both dosing routes. The major metabolite based on the peak area, M+16 (III) (Figure 2), was also detected in plasma samples. The previously unidentified metabolite seen *in vitro* (M–69) was also detected at very minor levels in the oral plasma samples.

Triazine 23 has high aqueous solubility (>100 µg/mL, Table 5), high permeability across Caco-2 cell monolayers (40×10^{-6} cm/s, Table 6), and physicochemical parameters that are within the ranges of compounds exhibiting good oral absorption; therefore, it seems unlikely that bioavailability is absorption limited. This is also consistent with the low fraction (2%) of the oral dose recovered in feces as an intact parent compound.

Additional mechanistic studies were conducted with 23 to understand the basis for the very high *in vivo* clearance. First, rats were administered 3 mg/kg 23 by intravenous infusion, following a predose with the pan CYP inhibitor, 1-aminobenzotriazine (ABT, see the SI for methods). Blood clearance in the ABT-treated rats was comparable to that observed in control animals (232 and 205 mL/min/kg, respectively), suggesting that CYP-mediated metabolism is not a predominant *in vivo* clearance process for 23 in rats. Second, the potential for the elimination of 23 by direct biliary excretion was evaluated in bile-cannulated rats. Only 0.1–0.2% of the IV dose of 23 was recovered in bile, indicating that 23 was not subject to biliary clearance to any meaningful extent. Further studies are ongoing to understand the processes contributing to the *in vivo* clearance of 23.

Overall, there remains a disconnect between the efficacy data and the low exposure of parent 23, although the possibility of a sex-based difference in exposure cannot be ruled out, as efficacy was assessed in female mice, whereas pharmacokinetic properties were defined in male mice. In terms of pharmacokinetics, the low recovery of compounds in rat urine and in bile suggests a minimal contribution of renal and biliary elimination. It seems likely that the high-clearance results from both hepatic metabolism and extrahepatic elimination routes that are yet to be defined. In terms of pharmacodynamics (PD), it cannot be ruled out that triazine 23 is fast-acting with a long duration of action even with rapid systemic clearance and low exposure. Alternatively, bioactive metabolites may contribute to this *in vivo* activity. We are currently assembling a range of diverse variants of triazine 23 to determine the origins of the PK–PD disconnect.

In Vivo Evaluation of Efficacy: 4-day Peters' Test in the *P. berghei*-Rodent Model. The second-generation 23 was evaluated in the Peters 4-day blood schizonticidal test as previously described.¹⁹ Following oral administration, the mean ED₅₀ and ED₉₀ values of 23 were 1.85 ± 0.37 and 4.10 ± 0.13 mg/kg/day, respectively. In contrast to the second-generation 23, the first-generation triazine 1 had ED₅₀ and ED₉₀ values of 1.47 ± 0.01 and 3.44 ± 0.40 mg/kg/day, respectively. For comparison purposes, the mean ED₅₀ values of artesunate and chloroquine are 1.37 ± 0.63 and 1.15 ± 0.06 mg/kg/day, respectively. No adverse events, such as loss of mobility or poor posture, were observed for 23 at the highest dose tested of 32 mg/kg/day for 4 days. From this study, it can be seen that despite its poor systemic exposure after oral dosing, 23 displayed excellent oral efficacy in this rodent malaria infection model.

In Vivo Evaluation of Efficacy: 4-day Peters' Test in the 3D7 Severe Combined Immunodeficient Mice (SCID) Mouse Model. Triazine 23 was next evaluated for its *in vivo* efficacy against *P. falciparum* in a 4-day model using humanized NOD-SCID IL2R γ^{null} mice.^{32,33} These mice can be engrafted daily with human erythrocytes as they are immunodeficient. The mice are then inoculated with *Pf* 3D7^{0087/N9}, with the compound being administered for 4 consecutive days from the 3rd day at a once-daily oral dosing of 50 mg/kg (Figure 7). It was observed that triazine 23 induced clearance of parasites from peripheral blood within 3 days of dosing.

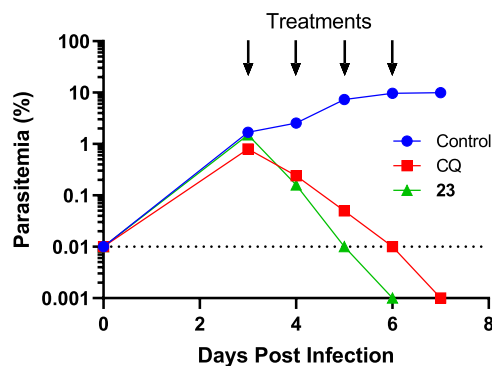


Figure 7. Efficacy of 23 against *P. falciparum* Pf3D70087/N9: *Pf* acute *in vivo* model, 4-day test by Peters. The arrows indicate the days of treatment (50 mg/kg PO) in the 4-day test by Peters. Values correspond to the average parasitemia in the peripheral blood of $n = 2$ mice/group.

The concentrations of triazine 23 in blood after oral administration were measured in serial blood samples obtained 1, 2, 4, 6, and 24 h following the first dosing in all compound-treated mice. Blood levels were measured at Swiss BioQuant (Basel, Switzerland) by liquid chromatography (LC)-MS/MS. Exposure of triazine 23 in this model was low with concentrations in the range of 150–250 ng/mL for ~6 h. By 24 h, concentrations were below the quantitation limit (Figure 8). The basis for the differences in exposure between the SCID mouse study (50 mg/kg PO) and the PK study (27 mg/kg PO) remains unclear.

CONCLUSIONS

The major limitations of our previously identified triazine 1 were poor PK properties (*i.e.*, low exposure) and toxicity alerts

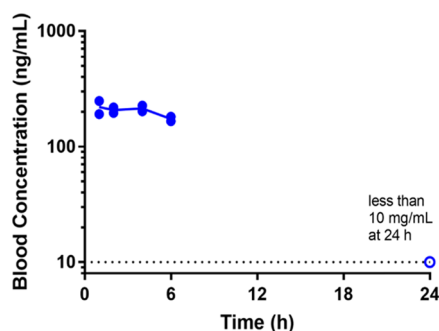


Figure 8. Mean ($n = 2$) blood concentrations of **23** after oral administration of 50 mg/kg to SCID mice.

associated with activated thioethers, which would limit the progression of this compound. To address this limitation, new SAR investigations led to the discovery of novel 3,3'-disubstituted-5,5'-bi(1,2,4-triazine) derivatives with potent *in vitro* activity against *P. falciparum* parasites. These second-generation bis-triazines identified simple structural modifications that led to enhanced microsomal stability, good solubility, and permeability while maintaining potency, which is exemplified by triazine **23** with an IC_{50} value of 31 nM in *Pf* 3D7 parasites. However, these favorable *in vitro* properties did not translate to an improved exposure profile *in vivo* and very high clearance remains a key issue for this series.

Triazine **23** was also evaluated in the PRR model (two-point FACS), where it demonstrated a fast-killing profile similar to that of both artesunate and chloroquine, and when assessed against a panel of laboratory strains with mutations in recently identified targets, **23** was observed to be equipotent against all strains tested, indicating that this substrate is acting *via* a novel mechanism of action. Furthermore, in the 4-day Peters test in the 3D7 SCID mouse model, it was observed that triazine **23** induced clearance of parasites from peripheral blood within 3 days of dosing.

The improved microsomal stability of the new compounds with comparable oral efficacy to **1** despite lower *in vitro* potency and poor systemic exposure is suggestive that this class of orally active antimalarial bis-triazines can be further optimized to improve the bioavailability, to afford a promising preclinical candidate, and we will report on these efforts in due course.

EXPERIMENTAL SECTION

Chemistry. *General Experimental Methods.* For all synthetic reactions, commercially available reagents were used without further purification. Column chromatography was performed using silica gel (40–60 μ m). The solvents utilized for chromatography were used as supplied without purification. Predominantly, the reactions were monitored by thin-layer chromatography (TLC) on Silica Gel 60_{F-254} plates with detection by UV light and/or $KMnO_4$ stain.

Purity. The purity of all compounds subjected for biological testing was >95%, as determined using the methods described below.

NMR. 1H and ^{13}C NMR spectra were recorded at 400 and 101 MHz, respectively, on a Bruker Avance III Nanobay spectrometer. NMR solvents were obtained from Cambridge Isotope Laboratories. Chemical shifts (δ , ppm) are reported relative to the solvent peak ($CDCl_3$), 7.26 ppm [1H] or 77.16 ppm [^{13}C]. Proton resonances are assigned as chemical shift (δ), multiplicity (s, singlet; d, doublet; m, multiplet), coupling constant (J , Hz), and the number of protons.

LC/MS. Low-resolution mass spectrometry analyses were performed on either (i) Agilent 6100 series single quad LC/MS coupled with an Agilent 1200 series high-performance liquid chromatography

(HPLC), 1200 series G1311A quaternary pump, 1200 series G1329A thermostated autosampler, and 1200 series G1314B variable wavelength detector. The conditions for liquid chromatography were: reverse-phase HPLC analysis fitted with a Phenomenex Luna C8(2) 5 μ m (50 mm \times 4.6 mm) 100 \AA column; column temperature, 30 $^\circ$ C; injection volume, 5 μ L; solvent, 99.9% acetonitrile, 0.1% formic acid; gradient, 5–100% of solvent over 10 min; and detection, 254 nm. The conditions for mass spectrometry were: a quadrupole ion source; ion mode, multimode-ES; drying gas temp, 300 $^\circ$ C; vaporizer temperature, 200 $^\circ$ C; capillary voltage, 2000 V (positive), 4000 V (negative); scan range, 100–1000 m/z ; step size, 0.1 s; acquisition time, 10 min; or (ii) an Agilent UHPLC-MS 1260/6120 system with the following technical information. Pump, 1260 Infinity G1312B binary pump; autosampler, 1260 Infinity G1367E 1260 HiP ALS; and detector, 1290 Infinity G4212A 1290 DAD. LC conditions: reverse-phase HPLC analysis; column, Poroshell 120 EC-C18 3.0 mm \AA to 50 mm 2.7 μ m; column temperature, 35 $^\circ$ C; injection volume, 1 μ L; and flow rate, 1 mL/min. Solvent A: 99.9% water and 0.1% formic acid. Solvent B: 99.9% acetonitrile and 0.1% formic acid, gradient 5–100% of solvent B in solvent A over 3.8 min. Gradient takes 4 min to get to 100% solvent B in solvent A, maintain for 3 min, and a further 3 min to get back to the original 5% solvent B in solvent A. MS conditions: an ion source, quadrupole; ion mode, atmospheric pressure ionization-electrospray (API-ES); drying gas temp, 350 $^\circ$ C; capillary voltage (V), 3000 (positive); capillary voltage (V), 3000 (negative); scan 52 range, 100–1000; step size, 0.1 s; and acquisition time, 5 min.

HRMS. High-resolution MS was performed with an Agilent 6224 TOF LC/MS coupled to an Agilent 1290 Infinity LC. All data were acquired, and reference mass corrected *via* a dual-spray electrospray ionization (ESI) source. Each scan or data point on the total ion chromatogram (TIC) is an average of 13 700 transients, producing a spectrum every second. Mass spectra were obtained by averaging the scans across each peak and subtracting the background from the first 10 s of the TIC. Acquisition was performed using the Agilent Mass Hunter data acquisition software ver. B.05.00 build 5.0.5042.2, and analysis was performed using Mass Hunter Qualitative Analysis ver. B.05.00 build 5.0.519.13. Acquisition parameters: mode, ESI; drying gas flow, 11 L/min; nebulizer pressure, 45 psi; and drying gas temperature, 325 $^\circ$ C. Voltages: capillary, 4000 V; fragmentor, 160 V; skimmer, 65 V; octapole RF, 750 V; scan range, 100–1500 m/z ; and positive ion mode internal reference ions, m/z 121.050873 and 922.009798. LC conditions: Agilent Zorbax SB-C18 Rapid Resolution HT (2.1 mm \AA to 50 mm, 1.8 mm column), 30 $^\circ$ C; sample (5 μ L) was eluted using a binary gradient (solvent A, 0.1% aq formic acid; solvent B, 0.1% formic acid in acetonitrile; 5–100% B [3.5 min], 0.5 mL/min).

Interference Compounds. All final compounds have been examined for the presence of substructures classified as Pan Assay Interference Compounds (PAINS) using a KNIME workflow.^{34,35}

General Synthetic Procedures. Triazines of three classes were used in the cyanide-mediated dimerization process, namely, 3-(alkylthio)-1,2,4-triazines, 3-(alkoxy)-1,2,4-triazines, and 3-(alkyl)-1,2,4-triazines. The synthesis of each class has been previously described by us or others in the literature. The synthesis of 3,3'-disubstituted-5,5'-bi(1,2,4-triazine)s **9–39** was accomplished using appropriate mixtures of 1,2,4-triazine monomers and potassium cyanide for coupling reactions as described previously by Courcot et al. and our group.^{19,21} While completing the synthesis of heterodimers, homodimers of each monomer were also obtained. Characterization data of the monomeric 1,2,4-triazines and dimeric 3,3'-disubstituted-5,5'-bi(1,2,4-triazine)s not previously described in the literature are outlined below.

3-((3-Azidopropyl)thio)-1,2,4-triazine (4a). Isolated as a brown oil in 77% yield. 1H NMR (400 MHz, $CDCl_3$) δ 8.94 (d, $J = 2.3$ Hz, 1H), 8.38 (d, $J = 2.3$ Hz, 1H), 3.48 (t, $J = 6.6$ Hz, 2H), 3.34–3.30 (m, 2H), 2.07 (dd, $J = 13.5, 6.6$ Hz, 2H) ppm. ^{13}C NMR (101 MHz, $CDCl_3$) δ 174.0, 148.4, 145.6, 50.2, 28.5, 27.8 ppm. MS (m/z) 197.0 [M + H]⁺.

3-(Prop-2-yn-1-ylthio)-1,2,4-triazine (4b). Isolated as a brown oil in 37% yield. 1H NMR (400 MHz, $CDCl_3$) δ 8.98 (d, $J = 2.4$ Hz, 1H), 8.43 (d, $J = 2.4$ Hz, 1H), 4.01 (d, $J = 2.6$ Hz, 2H), 2.22 (t, $J = 2.6$ Hz,

1H) ppm. ^{13}C NMR (101 MHz, CDCl_3) δ 172.8, 148.4, 145.9, 78.6, 71.4, 19.3 ppm. MS (m/z) 152.0 $[\text{M} + \text{H}]^+$.

3-Butyl-1,2,4-triazine (6a). Isolated as a yellow oil in 70% yield. ^1H NMR (400 MHz, CDCl_3) δ 9.09–9.08 (m, 1H), 8.54–8.53 (m, 1H), 3.14–3.09 (m, 2H), 1.88–1.80 (m, 2H), 1.44–1.37 (m, 2H), 0.96–0.91 (m, 3H) ppm. ^{13}C NMR (101 MHz, CDCl_3) δ 171.0, 148.8, 147.6, 37.2, 30.6, 22.5, 13.9 ppm. MS (m/z) 138.3 $[\text{M} + \text{H}]^+$.

General Method A. Solid KCN (3.7 equiv) was added to a solution of monomer A (1.0 equiv) and monomer B (1.0 equiv) in water (10 mL) and the solution was stirred at 40 °C for 1.5 h. The aqueous solution was then extracted with diethyl ether (3 \times 50 mL). The combined ether phases were dried over anhydrous MgSO_4 and the solvent was evaporated. The residue was purified by column chromatography on silica gel to afford the desired compounds.

2-((3'-(Isopropylthio)-[5,5'-bi(1,2,4-triazin)]-3-yl)thio)-N,N-dimethylethanamine (9). Prepared according to General Method A. The title compound was isolated as a brown solid in 28% yield. ^1H NMR (400 MHz, CDCl_3) δ 9.84 (s, 1H), 9.83 (s, 1H), 4.28–4.04 (m, 1H), 3.48 (t, $J = 7.0$ Hz, 2H), 2.75 (t, $J = 7.0$ Hz, 2H), 2.34 (s, 6H), 1.52 (d, $J = 6.8$ Hz, 6H) ppm. ^{13}C NMR (101 MHz, CDCl_3) δ 174.5, 174.2, 150.1, 145.0, 142.1, 141.8, 57.7, 45.3, 36.4, 29.0, 22.7 ppm. MS (m/z) 338.2 $[\text{M} + \text{H}]^+$. MP: 98.9–101.8 °C.

2-((3'-(2-Methoxyethylthio)-[5,5'-bi(1,2,4-triazin)]-3-yl)thio)-N,N-dimethylethanamine (10). Prepared according to General Method A. The title compound was isolated as a brown oil in 4% yield. ^1H NMR (400 MHz, CDCl_3) δ 9.89 (s, 1H), 9.87 (s, 1H), 3.78 (t, $J = 6.2$ Hz, 2H), 3.58 (t, $J = 6.2$ Hz, 2H), 3.52 (t, $J = 7.0$ Hz, 2H), 3.43 (s, 3H), 2.80 (t, $J = 7.0$ Hz, 2H), 2.38 (s, 6H) ppm. ^{13}C NMR (101 MHz, CDCl_3) δ 173.2, 172.9, 149.0, 148.9, 141.2, 141.1, 69.3, 57.9, 56.6, 44.2, 29.6, 27.9 ppm. MS (m/z) 354.1 $[\text{M} + \text{H}]^+$.

2-((3'-Methoxy-[5,5'-bi(1,2,4-triazin)]-3-yl)thio)-N,N-dimethylethanamine (11). Prepared according to General Method A. The title compound was isolated as a brown oil in 7% yield. ^1H NMR (400 MHz, CDCl_3) δ 9.91 (s, 1H), 9.89 (s, 1H), 4.30 (s, 3H), 3.49 (t, $J = 7.0$ Hz, 2H), 2.77 (t, $J = 7.0$ Hz, 2H), 2.35 (s, 6H) ppm. ^{13}C NMR (101 MHz, CDCl_3) δ 174.2, 165.5, 152.8, 145.0, 142.1, 141.7, 56.5, 56.5, 45.3, 28.9 ppm. MS (m/z) 294.2 $[\text{M} + \text{H}]^+$.

N,N-Dimethyl-2-((3'-propoxy-[5,5'-bi(1,2,4-triazin)]-3-yl)thio)-ethanamine (12). Prepared according to General Method A. The title compound was isolated as a brown solid in 17% yield. ^1H NMR (400 MHz, CDCl_3) δ 9.91 (s, 1H), 9.90 (s, 1H), 4.62 (t, $J = 6.7$ Hz, 2H), 3.49 (t, $J = 7.0$ Hz, 2H), 2.76 (t, $J = 7.0$ Hz, 2H), 2.35 (s, 6H), 2.06–1.89 (m, 2H), 1.11 (t, $J = 7.4$ Hz, 3H) ppm. ^{13}C NMR (101 MHz, CDCl_3) δ 174.2, 165.3, 152.7, 150.1, 142.2, 141.5, 71.2, 57.7, 45.3, 29.0, 22.1, 10.4 ppm. MS (m/z) 322.2 $[\text{M} + \text{H}]^+$. MP: 80.9–85.9 °C.

2-((3'-Isopropoxy-[5,5'-bi(1,2,4-triazin)]-3-yl)thio)-N,N-dimethylethanamine (13). Prepared according to General Method A. The title compound was isolated as a brown solid in 3% yield. ^1H NMR (400 MHz, CDCl_3) δ 9.89 (s, 1H), 9.89 (s, 1H), 5.71–5.54 (m, 1H), 3.51 (t, $J = 7.1$ Hz, 2H), 2.80 (t, $J = 7.1$ Hz, 2H), 2.38 (s, 6H), 1.53 (d, $J = 6.2$ Hz, 6H) ppm. ^{13}C NMR (101 MHz, CDCl_3) δ 174.1, 164.8, 152.7, 150.2, 142.2, 141.2, 73.2, 57.6, 45.2, 28.8, 21.7 ppm. MS (m/z) 322.2 $[\text{M} + \text{H}]^+$. MP: 60.1–62.1 °C.

2-((3'-Ethyl-[5,5'-bi(1,2,4-triazin)]-3-yl)thio)-N,N-dimethylethanamine (15). Prepared according to General Method A. The title compound was isolated as a yellow solid in 15% yield. ^1H NMR (400 MHz, CDCl_3) δ 10.08 (s, 1H), 9.96 (s, 1H), 3.50 (t, $J = 6.8$ Hz, 2H), 3.31 (dd, $J = 14.8, 7.4$ Hz, 2H), 2.76 (t, $J = 6.7$ Hz, 2H), 2.35 (s, 6H), 1.51 (t, $J = 7.4$ Hz, 3H) ppm. ^{13}C NMR (101 MHz, CDCl_3) δ 174.3, 171.3, 150.6, 150.5, 144.5, 142.3, 57.9, 45.4, 30.7, 29.2, 12.4 ppm. MS (m/z) 292.2 $[\text{M} + \text{H}]^+$. MP: 87–89 °C.

2-((3'-Butyl-[5,5'-bi(1,2,4-triazin)]-3-yl)thio)-N,N-dimethylethanamine (16). Prepared according to General Method A. The title compound was isolated as a yellow solid in 28% yield. ^1H NMR (400 MHz, CDCl_3) δ 10.07 (s, 1H), 9.95 (s, 1H), 3.50 (t, $J = 7.0$ Hz, 2H), 3.38–3.17 (m, 2H), 2.77 (t, $J = 7.0$ Hz, 2H), 2.35 (s, 6H), 2.05–1.84 (m, 2H), 1.58–1.36 (m, 2H), 0.99 (t, $J = 7.4$ Hz, 3H) ppm. ^{13}C NMR (101 MHz, CDCl_3) δ 174.3, 170.7, 150.6, 150.5, 144.4, 142.3, 57.9, 45.4, 37.0, 30.5, 29.1, 22.5, 13.9 ppm. MS (m/z) 320.3 $[\text{M} + \text{H}]^+$. MP: 51–53 °C.

3-(Methylthio)-3'-(prop-2-yn-1-ylthio)-5,5'-bi(1,2,4-triazine) (17). Prepared according to General Method A. The title compound was isolated as a yellow solid in 22% yield. ^1H NMR (400 MHz, CDCl_3) δ 9.95 (s, 1H), 9.93 (s, 1H), 4.08 (d, $J = 2.6$ Hz, 2H), 2.77 (s, 3H), 2.25 (t, $J = 2.6$ Hz, 1H) ppm. ^{13}C NMR (101 MHz, CDCl_3) δ 174.6, 172.7, 150.4, 149.8, 142.6, 142.2, 78.2, 71.7, 19.7, 14.2 ppm. MS (m/z) 277.1 $[\text{M} + \text{H}]^+$, HRMS (m/z) calcd $\text{C}_{10}\text{H}_8\text{N}_6\text{S}_2$ $[\text{M} + \text{H}]^+$ 277.0325; found 277.0329. MP: 125–127 °C.

3-((3-Azidopropylthio)-3'-(methylthio)-5,5'-bi(1,2,4-triazine) (18). Prepared according to General Method A. The title compound was isolated as a yellow solid in 34% yield. ^1H NMR (400 MHz, CDCl_3) δ 9.91 (s, 1H), 9.90 (s, 1H), 3.54 (t, $J = 6.3$ Hz, 2H), 3.44 (t, $J = 7.0$ Hz, 2H), 2.77 (s, 3H), 2.27–1.99 (m, 2H) ppm. ^{13}C NMR (101 MHz, CDCl_3) δ 174.6, 173.8, 150.3, 149.9, 142.4, 142.1, 50.2, 28.4, 28.1, 14.2 ppm. MS (m/z) 322.1 $[\text{M} + \text{H}]^+$, HRMS (m/z) calcd $\text{C}_{10}\text{H}_{11}\text{N}_9\text{S}_2$ $[\text{M} + \text{H}]^+$ 322.0652; found 322.0655. MP: 67–69 °C.

N,N-Dimethyl-2-((3'-(methylthio)-[5,5'-bi(1,2,4-triazin)]-3-yl)oxy)propan-1-amine (20). Prepared according to General Method A. The title compound was isolated as a yellow solid in 34% yield. ^1H NMR (400 MHz, CDCl_3) δ 9.89 (s, 1H), 9.88 (s, 1H), 5.70 (m, 1H), 2.85 (dd, $J = 13.1, 7.9$ Hz, 1H), 2.75 (s, 3H), 2.48 (dd, $J = 13.1, 4.3$ Hz, 1H), 2.30 (s, 6H), 1.49 (d, $J = 6.2$ Hz, 3H) ppm. ^{13}C NMR (101 MHz, CDCl_3) δ 174.5, 165.2, 152.9, 150.1, 142.2, 141.5, 74.0, 64.6, 46.3, 18.2, 14.1 ppm. MS (m/z) 308.1 $[\text{M} + \text{H}]^+$, HRMS (m/z) calcd $\text{C}_{12}\text{H}_{17}\text{N}_7\text{OS}$ $[\text{M} + \text{H}]^+$ 308.1288; found 308.1277.

3-(Methylthio)-3'-(prop-2-yn-1-yloxy)-5,5'-bi(1,2,4-triazine) (21). Prepared according to General Method A. The title compound was isolated as a yellow solid in 41% yield. ^1H NMR (400 MHz, CDCl_3) δ 10.00 (s, 1H), 9.91 (s, 1H), 5.29 (d, $J = 2.1$ Hz, 2H), 2.76 (s, 1H), 2.59 (s, 3H) ppm. ^{13}C NMR (101 MHz, CDCl_3) δ 174.6, 164.4, 153.1, 149.8, 142.4, 142.2, 76.9, 76.4, 56.8, 14.2 ppm. MS (m/z) 261.1 $[\text{M} + \text{H}]^+$, HRMS (m/z) calcd $\text{C}_{10}\text{H}_8\text{N}_6\text{OS}$ $[\text{M} + \text{H}]^+$ 260.0475; found 260.0465. MP: 116–118 °C.

2-((3'-(Isopropylthio)-[5,5'-bi(1,2,4-triazin)]-3-yl)oxy)-N,N-dimethylethanamine (22). Prepared according to General Method A. The title compound was isolated as a brown solid in 7% yield. ^1H NMR (400 MHz, CDCl_3) δ 9.90 (s, 1H), 9.85 (s, 1H), 4.77 (t, $J = 5.6$ Hz, 2H), 4.14 (m, 1H), 2.90 (t, $J = 5.6$ Hz, 2H), 2.39 (s, 6H), 1.51 (d, $J = 6.8$ Hz, 6H) ppm. ^{13}C NMR (101 MHz, CDCl_3) δ 174.5, 165.1, 153.1, 149.9, 141.9, 141.8, 66.8, 57.5, 45.7, 36.5, 22.7 ppm. MS (m/z) 322.2 $[\text{M} + \text{H}]^+$. MP: 63.4–67.9 °C.

N,N-Dimethyl-2-((3'-propoxy-[5,5'-bi(1,2,4-triazin)]-3-yl)oxy)-ethanamine (23). Prepared according to General Method A. The title compound was isolated as a yellow solid in 19% yield. ^1H NMR (400 MHz, CDCl_3) δ 9.94 (s, 1H), 9.92 (s, 1H), 4.76 (t, $J = 5.6$ Hz, 2H), 4.61 (t, $J = 6.7$ Hz, 2H), 2.86 (t, $J = 5.6$ Hz, 2H), 2.36 (s, 6H), 2.08–1.82 (m, 2H), 1.10 (t, $J = 7.4$ Hz, 3H) ppm. ^{13}C NMR (101 MHz, CDCl_3) δ 165.3, 165.2, 153.1, 152.8, 141.9, 141.7, 71.3, 67.2, 57.8, 45.9, 22.2, 10.5 ppm. MS (m/z) 306.2 $[\text{M} + \text{H}]^+$. MP: 47–49 °C.

2-((3'-Isopropoxy-[5,5'-bi(1,2,4-triazin)]-3-yl)oxy)-N,N-dimethylethanamine (24). Prepared according to General Method A. The title compound was isolated as a yellow solid in 27% yield. ^1H NMR (400 MHz, CDCl_3) δ 9.93 (s, 1H), 9.89 (s, 1H), 5.59 (dq, $J = 11.7, 5.8$ Hz, 1H), 4.75 (t, $J = 5.5$ Hz, 2H), 2.85 (t, $J = 5.5$ Hz, 2H), 2.35 (s, 6H), 1.52 (d, $J = 6.1$ Hz, 6H) ppm. ^{13}C NMR (101 MHz, CDCl_3) δ 165.2, 164.8, 153.1, 152.8, 141.9, 141.4, 73.2, 67.2, 57.8, 45.9, 21.8 ppm. MS (m/z) 306.2 $[\text{M} + \text{H}]^+$. MP: 81–83 °C.

N,N-Dimethyl-2-((3'-(3,3,3-trifluoropropoxy)-[5,5'-bi(1,2,4-triazin)]-3-yl)oxy)ethanamine (25). Prepared according to General Method A. The title compound was isolated as a yellow oil in 21% yield. ^1H NMR (400 MHz, CDCl_3) δ 10.00 (s, 1H), 9.95 (s, 1H), 4.91 (t, $J = 6.4$ Hz, 2H), 4.78 (t, $J = 5.6$ Hz, 2H), 2.88 (t, $J = 5.6$ Hz, 2H), 2.85–2.75 (m, 2H), 2.38 (s, 6H) ppm. ^{13}C NMR (101 MHz, CDCl_3) δ 165.2, 164.7, 153.4, 152.7, 142.5, 141.9, 125.8 (q, $J = 276.6$ Hz), 67.3, 62.3 (d, $J = 3.8$ Hz), 57.8, 45.9, 33.7 (q, $J = 29.5$ Hz) ppm. ^{19}F NMR (376 MHz, CDCl_3) δ –64.77 ppm. MS (m/z) 360.2 $[\text{M} + \text{H}]^+$. MP: 50–52 °C.

2-((3'-Butyl-[5,5'-bi(1,2,4-triazin)]-3-yl)oxy)-N,N-dimethylethanamine (26). Prepared according to General Method A. The title compound was isolated as a yellow oil in 30% yield. ^1H NMR (400 MHz, CDCl_3) δ 10.08 (s, 1H), 10.00 (s, 1H), 4.77 (t, $J = 5.7$ Hz,

2H), 3.38–3.11 (m, 2H), 2.86 (t, $J = 5.7$ Hz, 2H), 2.37 (s, 6H), 2.02–1.79 (m, 2H), 1.57–1.36 (m, 2H), 0.98 (t, $J = 7.4$ Hz, 3H) ppm. ^{13}C NMR (101 MHz, CDCl_3) δ 170.6, 165.3, 153.6, 150.5, 144.5, 141.9, 67.2, 57.8, 45.9, 36.9, 30.5, 22.5, 13.9 ppm. MS (m/z) 304.3 $[\text{M} + \text{H}]^+$.

3,3'-Bis((3-azidopropyl)thio)-5,5'-bi(1,2,4-triazine) (27). Prepared according to General Method A. The title compound was isolated as a yellow solid in 27% yield. ^1H NMR (400 MHz, CDCl_3) δ 9.92 (s, 2H), 3.53 (t, $J = 6.3$ Hz, 4H), 3.43 (t, $J = 7.0$ Hz, 4H), 2.39–1.84 (m, 2H) ppm. ^{13}C NMR (101 MHz, CDCl_3) δ 173.8, 150.1, 142.4, 50.2, 28.4, 28.1 ppm. MS (m/z) 391.1 $[\text{M} + \text{H}]^+$. MP: 76–78 °C.

3,3'-Dibutyl-5,5'-bi(1,2,4-triazine) (28). Prepared according to General Method A. The title compound was isolated as a yellow solid in 50% yield. ^1H NMR (400 MHz, CDCl_3) δ 10.16 (s, 2H), 3.28 (t, $J = 7.7$ Hz, 4H), 2.03–1.84 (m, 4H), 1.49 (dq, $J = 14.7$, 7.3 Hz, 4H), 1.00 (t, $J = 7.3$ Hz, 6H) ppm. ^{13}C NMR (101 MHz, CDCl_3) δ 170.7, 151.1, 144.6, 37.0, 30.6, 22.5, 14.0 ppm. MS (m/z) 273.2 $[\text{M} + \text{H}]^+$. MP: 45–47 °C.

3,3'-Dipropoxy-5,5'-bi(1,2,4-triazine) (29). Prepared according to General Method A. The title compound was isolated as a yellow solid in 68% yield. ^1H NMR (400 MHz, CDCl_3) δ 9.96 (s, 2H), 4.64 (t, $J = 6.7$ Hz, 4H), 2.11–1.89 (m, 4H), 1.12 (t, $J = 7.4$ Hz, 6H) ppm. ^{13}C NMR (101 MHz, CDCl_3) δ 165.4, 152.9, 141.7, 71.4, 22.2, 10.5 ppm. MS (m/z) 277.2 $[\text{M} + \text{H}]^+$, HRMS (m/z) calcd $\text{C}_{12}\text{H}_{16}\text{N}_6\text{O}_2$ $[\text{M} + \text{H}]^+$ 277.1408; found 277.1406. MP: 96–98 °C.

3,3'-Diisopropoxy-5,5'-bi(1,2,4-triazine) (30). Prepared according to General Method A. The title compound was isolated as a yellow solid in 41% yield. ^1H NMR (400 MHz, CDCl_3) δ 9.92 (s, 2H), 5.72–5.52 (m, 2H), 1.55 (s, 6H), 1.54 (s, 6H) ppm. ^{13}C NMR (101 MHz, CDCl_3) δ 164.9, 153.1, 141.4, 73.3, 21.9 ppm. MS (m/z) 277.2 $[\text{M} + \text{H}]^+$. MP: 114–116 °C.

3,3'-Dicyclopropoxy-5,5'-bi(1,2,4-triazine) (31). Prepared according to General Method A. The title compound was isolated as a yellow solid in 29% yield. ^1H NMR (400 MHz, CDCl_3) δ 10.00 (s, 2H), 4.75–4.53 (m, 2H), 0.99 (s, 8H) ppm. ^{13}C NMR (101 MHz, CDCl_3) δ 166.4, 152.8, 142.2, 53.6, 6.2 ppm. MS (m/z) 273.2 $[\text{M} + \text{H}]^+$, HRMS (m/z) calcd $\text{C}_{12}\text{H}_{12}\text{N}_6\text{O}_2$ $[\text{M} + \text{H}]^+$ 273.1095; found 273.1097. MP: 137–139 °C.

3,3'-Bis(3,3,3-trifluoropropoxy)-5,5'-bi(1,2,4-triazine) (32). Prepared according to General Method A. The title compound was isolated as a yellow solid in 56% yield. ^1H NMR (400 MHz, CDCl_3) δ 10.02 (s, 2H), 4.93 (t, $J = 6.3$ Hz, 4H), 3.02–2.62 (m, 4H) ppm. ^{13}C NMR (101 MHz, CDCl_3) δ 164.7, 153.0, 142.5, 125.8 (q, $J = 276.7$ Hz), 62.4 (d, $J = 3.7$ Hz), 33.7 (q, $J = 29.6$ Hz) ppm. ^{19}F NMR (376 MHz, CDCl_3) δ –64.77 ppm. MS (m/z) 385.1 $[\text{M} + \text{H}]^+$. MP: 96–98 °C.

3,3'-Bis(2-(trimethylsilyl)ethoxy)-5,5'-bi(1,2,4-triazine) (33). Prepared according to General Method A. The title compound was isolated as a yellow solid in 24% yield. ^1H NMR (400 MHz, CDCl_3) δ 9.93 (s, 2H), 4.82–4.73 (m, 4H), 1.37–1.28 (m, 4H), 0.13 (s, 18H) ppm. ^{13}C NMR (101 MHz, CDCl_3) δ 165.2, 153.0, 141.6, 68.3, 17.7, –1.3 ppm. MS (m/z) 393.2 $[\text{M} + \text{H}]^+$, HRMS (m/z) calcd for $\text{C}_{16}\text{H}_{28}\text{N}_6\text{O}_2\text{Si}_2$ $[\text{M} + \text{H}]^+$ 393.1885; found 393.1883. MP: 91–93 °C.

3,3'-Bis(2,2,2-trifluoroethoxy)-5,5'-bi(1,2,4-triazine) (34). Prepared according to General Method A. The title compound was isolated as a yellow solid in 26% yield. ^1H NMR (400 MHz, CDCl_3) δ 10.11 (s, 2H), 5.12 (q, $J = 8.0$ Hz, 4H) ppm. ^{13}C NMR (101 MHz, CDCl_3) δ 164.0, 153.1, 143.3, 122.8 (q, $J = 277.5$ Hz), 65.0 (q, $J = 37.3$ Hz) ppm. MS (m/z) 357.1 $[\text{M} + \text{H}]^+$. MP: 157–159 °C.

3,3'-Bis(2-methoxyethoxy)-5,5'-bi(1,2,4-triazine) (35). Prepared according to General Method A. The title compound was isolated as a yellow solid in 42% yield. ^1H NMR (400 MHz, CDCl_3) δ 9.97 (s, 2H), 5.06–4.70 (m, 4H), 4.08–3.68 (m, 4H), 3.47 (s, 6H) ppm. ^{13}C NMR (101 MHz, CDCl_3) δ 165.2, 153.0, 142.1, 70.3, 68.6, 59.3 ppm. MS (m/z) 309.2 $[\text{M} + \text{H}]^+$, HRMS (m/z) calcd for $\text{C}_{12}\text{H}_{16}\text{N}_6\text{O}_4$ $[\text{M} + \text{H}]^+$ 309.1306; found 309.1297. MP: 104–106 °C.

3,3'-Bis(2-(4-methylthiazol-5-yl)ethoxy)-5,5'-bi(1,2,4-triazine) (36). Prepared according to General Method A. The title compound was isolated as a yellow solid in 43% yield. ^1H NMR (400 MHz, CDCl_3) δ 9.96 (s, 2H), 8.61 (s, 2H), 4.84 (t, $J = 6.3$ Hz, 4H), 3.42 (t,

$J = 6.2$ Hz, 4H), 2.47 (s, 6H) ppm. ^{13}C NMR (101 MHz, CDCl_3) δ 165.0, 152.9, 150.5, 150.3, 142.1, 126.1, 69.0, 26.1, 15.1 ppm. HRMS (m/z) calcd for $\text{C}_{18}\text{H}_{18}\text{N}_8\text{O}_2\text{S}_2$ $[\text{M} + \text{H}]^+$ 443.1067; found 443.1075. MP: 168–170 °C.

2,2'-((5,5'-Bi(1,2,4-triazine))-3,3'-diylbis(oxy))bis(N,N-dimethylthalamine) (37). Prepared according to General Method A. The title compound was isolated as a yellow solid in 27% yield. ^1H NMR (400 MHz, CDCl_3) δ 9.95 (s, 2H), 4.78 (t, $J = 5.6$ Hz, 4H), 2.87 (t, $J = 5.6$ Hz, 4H), 2.38 (s, 12H) ppm. ^{13}C NMR (101 MHz, CDCl_3) δ 165.2, 153.0, 142.0, 67.3, 57.9, 46.0 ppm. MS (m/z) 335.3 $[\text{M} + \text{H}]^+$. MP: 80–82 °C.

2,2'-((5,5'-Bi(1,2,4-triazine))-3,3'-diylbis(oxy))bis(N,N-dimethylpropan-1-amine) (38). Prepared according to General Method A. The title compound was isolated as a yellow oil in 30% yield. ^1H NMR (400 MHz, CDCl_3) δ 9.90 (s, 2H), 5.79–5.56 (m, 2H), 2.84 (dd, $J = 13.1$, 7.9 Hz, 2H), 2.48 (dd, $J = 13.1$, 4.4 Hz, 2H), 2.31 (s, 12H), 1.48 (t, $J = 5.6$ Hz, 6H) ppm. ^{13}C NMR (101 MHz, CDCl_3) δ 165.2, 153.0, 141.6, 139.2, 73.9, 64.6, 46.3, 18.2 ppm. MS (m/z) 363.3 $[\text{M} + \text{H}]^+$.

3,3'-Bis(prop-2-yn-1-yloxy)-5,5'-bi(1,2,4-triazine) (39). Prepared according to General Method A. The title compound was isolated as a yellow solid in 46% yield. ^1H NMR (400 MHz, CDCl_3) δ 10.05 (s, 2H), 5.31 (d, $J = 2.3$ Hz, 4H), 2.60 (t, $J = 2.3$ Hz, 2H) ppm. ^{13}C NMR (101 MHz, CDCl_3) δ 164.5, 152.9, 142.5, 76.9, 76.5, 56.9 ppm. MS (m/z) 269.1 $[\text{M} + \text{H}]^+$. MP: 102–104 °C.

■ ASSOCIATED CONTENT

Supporting Information

The Supporting Information is available free of charge at <https://pubs.acs.org/doi/10.1021/acs.jmedchem.1c00044>.

Structural biology methods are provided (PDF)

SMILES strings are listed for all new compounds tested (CSV)

■ AUTHOR INFORMATION

Corresponding Author

Jonathan B. Baell – Medicinal Chemistry, Monash Institute of Pharmaceutical Sciences, Monash University (Parkville Campus), Parkville, VIC 3052, Australia; ARC Centre for Fragment-Based Design, Monash University (Parkville Campus), Parkville, VIC 3052, Australia; orcid.org/0000-0003-2114-8242; Email: jonathan.baell@monash.edu

Authors

Daniel L. Priebsenow – School of Chemistry, The University of Melbourne, Parkville, VIC 3010, Australia; orcid.org/0000-0002-7840-0405

Mitch Mathiew – Medicinal Chemistry, Monash Institute of Pharmaceutical Sciences, Monash University (Parkville Campus), Parkville, VIC 3052, Australia

Da-Hua Shi – Medicinal Chemistry, Monash Institute of Pharmaceutical Sciences, Monash University (Parkville Campus), Parkville, VIC 3052, Australia

Jitendra R. Harjani – Medicinal Chemistry, Monash Institute of Pharmaceutical Sciences, Monash University (Parkville Campus), Parkville, VIC 3052, Australia

Julia G. Beveridge – Medicinal Chemistry, Monash Institute of Pharmaceutical Sciences, Monash University (Parkville Campus), Parkville, VIC 3052, Australia

Marina Chavchich – The Department of Drug Evaluation, Australian Defence Force Malaria and Infectious Disease Institute, Brisbane, QLD 4051, Australia

Michael D. Edstein – The Department of Drug Evaluation, Australian Defence Force Malaria and Infectious Disease Institute, Brisbane, QLD 4051, Australia

Sandra Duffy – Discovery Biology and School of Environment & Science, Griffith University, Nathan, QLD 4111, Australia

Vicky M. Avery – Discovery Biology and School of Environment & Science, Griffith University, Nathan, QLD 4111, Australia

Robert T. Jacobs – Medicines for Malaria Venture (MMV), CH-1215 Geneva, Switzerland

Stephen Brand – Medicines for Malaria Venture (MMV), CH-1215 Geneva, Switzerland

David M. Shackleford – Centre for Drug Candidate Optimisation, Monash Institute of Pharmaceutical Sciences, Monash University (Parkville Campus), Parkville, VIC 3052, Australia

Wen Wang – Centre for Drug Candidate Optimisation, Monash Institute of Pharmaceutical Sciences, Monash University (Parkville Campus), Parkville, VIC 3052, Australia

Longjin Zhong – Centre for Drug Candidate Optimisation, Monash Institute of Pharmaceutical Sciences, Monash University (Parkville Campus), Parkville, VIC 3052, Australia

Given Lee – Centre for Drug Candidate Optimisation, Monash Institute of Pharmaceutical Sciences, Monash University (Parkville Campus), Parkville, VIC 3052, Australia

Erin Tay – Centre for Drug Candidate Optimisation, Monash Institute of Pharmaceutical Sciences, Monash University (Parkville Campus), Parkville, VIC 3052, Australia

Helena Barker – Centre for Drug Candidate Optimisation, Monash Institute of Pharmaceutical Sciences, Monash University (Parkville Campus), Parkville, VIC 3052, Australia

Elly Crighton – Centre for Drug Candidate Optimisation, Monash Institute of Pharmaceutical Sciences, Monash University (Parkville Campus), Parkville, VIC 3052, Australia

Karen L. White – Centre for Drug Candidate Optimisation, Monash Institute of Pharmaceutical Sciences, Monash University (Parkville Campus), Parkville, VIC 3052, Australia

Susan A. Charman – Centre for Drug Candidate Optimisation, Monash Institute of Pharmaceutical Sciences, Monash University (Parkville Campus), Parkville, VIC 3052, Australia

Amanda De Paoli – Drug Delivery Disposition and Dynamics, Monash Institute of Pharmaceutical Sciences, Monash University (Parkville Campus), Parkville, VIC 3052, Australia

Darren J. Creek – Drug Delivery Disposition and Dynamics, Monash Institute of Pharmaceutical Sciences, Monash University (Parkville Campus), Parkville, VIC 3052, Australia; orcid.org/0000-0001-7497-7082

Complete contact information is available at:

<https://pubs.acs.org/10.1021/acs.jmedchem.1c00044>

Author Contributions

D.L.P. and M.M. were involved in chemical synthesis and manuscript preparation and D.-H.S., J.R.H., and J.G.B. assisted with chemical synthesis. M.C., M.D.E., S.D., V.M.A., R.T.J., and

S.B. all made key contributions to the array of biological testing and analysis required. D.M.S., W.W., L.Z., G.L., E.T., H.B., E.C., K.L.W., and S.A.C. generated and interpreted the ADME and PK data, and S.A.C. and D.M.S. contributed to manuscript preparation. A.D.P. and D.J.C. generated and interpreted the MTT assay data. J.B.B. was involved in leading and directing the overall program and writing the manuscript.

Notes

The authors declare no competing financial interest.

ACKNOWLEDGMENTS

D.L.P. acknowledges funding support from the Australian Research Council (DE200100949). The National Health and Medical Research Council of Australia (NHMRC) is thanked for Research Support (#1030704, 1080146) and Fellowship support for J.B.B. (2012–2016 Senior Research Fellowship #1020411, 2017—Principal Research Fellowship #1117602). This work was also supported by an NHMRC Synergy grant (#1185354). Also acknowledged are the Australian Federal Government Education Investment Fund Super Science Initiative and the Victorian State Government, Victoria Science Agenda Investment Fund for infrastructure support and the facilities and the scientific and technical assistance of the Australian Translational Medicinal Chemistry Facility (ATMCF), Monash Institute of Pharmaceutical Sciences (MIPS). ATMCF and the Center for Drug Candidate Optimisation (CDCO) are supported by Therapeutic Innovation Australia (TIA). TIA is supported by the Australian Government through the National Collaborative Research Infrastructure Strategy (NCRIS) program. Delphine Baud, Maelle Duffey, and Virginia Crivelli are acknowledged for their contributions to the coordination of the various studies at MMV partner facilities. Technical assistance from Jaya Jayaseelan, Golnar Golbaghi, and Meiyu Hu is also gratefully acknowledged. The ongoing support of the MMV to VMA is also acknowledged. We are grateful to Kerryn Rowcliffe for technical support in *in vitro* drug susceptibility assays and thank the Australian Red Cross Blood Service for the provision of human blood, plasma, and sera for *in vitro* cultivation of *P. falciparum* lines at Monash University, ADFMIDI, and Griffith University. We also thank Karin Van Breda, Ivor Harris, Anthony Kent, and Stephen McLeod-Robertson for the *in vivo* efficacy testing of **23** in the *P. berghei*-rodent model. The views expressed in this article are those of the authors and do not necessarily reflect those of the Australian Defence Force Joint Health Command or any extant Australian Defence Force policy.

ABBREVIATIONS

ED₅₀, half effective dose; SAR, structure–activity relationship; DMF, *N,N*-dimethylformamide; MeCN, acetonitrile; rt, room temperature; EtOH, ethanol; LHS, left hand side; RHS, right hand side; *Pf*, *Plasmodium falciparum*; *P.*, *Plasmodium*; Me, methyl; Et, ethyl; ⁿBu, *n*-butyl; ⁱPr, isopropyl; ⁿPr, *n*-propyl; ^oPr, cyclopropyl; ADMET, absorption, distribution, metabolism, excretion and toxicity; CL_{int}, intrinsic clearance; E_H, hepatic extraction ratio; IC₅₀, half-maximal inhibitory concentration; RBC, red blood cells; PRR, parasite reduction rate; HLM, human liver microsomes; MLM, mouse liver microsomes; PK, Pharmacokinetics; MW, molecular weight; PSA, polar surface area; TLC, thin-layer chromatography; UV, ultraviolet

■ REFERENCES

- (1) World Malaria Report 2019; World Health Organization: Geneva, 2019. www.who.int/malaria/publications/world-malaria-report-2019/en/ (accessed Feb 16, 2021).
- (2) Phillips, M. A.; Burrows, J. N.; Manyando, C.; van Huijsdijnen, R. H.; Van Voorhis, W. C.; Wells, T. N. C. Malaria. *Nat. Rev. Dis. Primers* **2017**, *3*, No. 17050.
- (3) Okombo, J.; Chibale, K. Recent updates in the discovery and development of novel antimalarial drug candidates. *MedChemComm* **2018**, *9*, 437–453.
- (4) Phillips, M. A.; Gujjar, R.; Malmquist, N. A.; White, J.; El Mazouni, F.; Baldwin, J.; Rathod, P. K. Triazolopyrimidine-Based Dihydroorotate Dehydrogenase Inhibitors with Potent and Selective Activity against the Malaria Parasite *Plasmodium falciparum*. *J. Med. Chem.* **2008**, *51*, 3649–3653.
- (5) Gujjar, R.; El Mazouni, F.; White, K. L.; White, J.; Creason, S.; Shackelford, D. M.; Deng, X.; Charman, W. N.; Bathurst, I.; Burrows, J.; Floyd, D. M.; Matthews, D.; Buckner, F. S.; Charman, S. A.; Phillips, M. A.; Rathod, P. K. Lead Optimization of Aryl and Aralkyl Amine-Based Triazolopyrimidine Inhibitors of *Plasmodium falciparum* Dihydroorotate Dehydrogenase with Antimalarial Activity in Mice. *J. Med. Chem.* **2011**, *54*, 3935–3949.
- (6) Gujjar, R.; Marwaha, A.; El Mazouni, F.; White, J.; White, K. L.; Creason, S.; Shackelford, D. M.; Baldwin, J.; Charman, W. N.; Buckner, F. S.; Charman, S.; Rathod, P. K.; Phillips, M. A. Identification of a Metabolically Stable Triazolopyrimidine-Based Dihydroorotate Dehydrogenase Inhibitor with Antimalarial Activity in Mice. *J. Med. Chem.* **2009**, *52*, 1864–1872.
- (7) Deng, X.; Kokkonda, S.; El Mazouni, F.; White, J.; Burrows, J. N.; Kaminsky, W.; Charman, S. A.; Matthews, D.; Rathod, P. K.; Phillips, M. A. Fluorine Modulates Species Selectivity in the Triazolopyrimidine Class of *Plasmodium falciparum* Dihydroorotate Dehydrogenase Inhibitors. *J. Med. Chem.* **2014**, *57*, 5381–5394.
- (8) Phillips, M. A.; Lotharius, J.; Marsh, K.; White, J.; Dayan, A.; White, K. L.; Njoroge, J. W.; El Mazouni, F.; Lao, Y.; Kokkonda, S.; Tomchick, D. R.; Deng, X.; Laird, T.; Bhatia, S. N.; March, S.; Ng, C. L.; Fidock, D. A.; Wittlin, S.; Lafuente-Monasterio, M.; Benito, F. J. G.; Alonso, L. M. S.; Martinez, M. S.; Jimenez-Diaz, M. B.; Bazaga, S. F.; Angulo-Barturen, I.; Haselden, J. N.; Louttit, J.; Cui, Y.; Sridhar, A.; Zeeman, A.-M.; Kocken, C.; Sauerwein, R.; Decherig, K.; Avery, V. M.; Duffy, S.; Delves, M.; Sinden, R.; Ruecker, A.; Wickham, K. S.; Rochford, R.; Gahagen, J.; Iyer, L.; Riccio, E.; Mirsalis, J.; Bathhurst, I.; Rueckle, T.; Ding, X.; Campo, B.; Leroy, D.; Rogers, M. J.; Rathod, P. K.; Burrows, J. N.; Charman, S. A. A long-duration dihydroorotate dehydrogenase inhibitor (DSM265) for prevention and treatment of malaria. *Sci. Transl. Med.* **2015**, *7*, No. 296ra111.
- (9) Plouffe, D.; Brinker, A.; McNamara, C.; Henson, K.; Kato, N.; Kuhlen, K.; Nagle, A.; Adrián, F.; Matzen, J. T.; Anderson, P.; Nam, T.-g.; Gray, N. S.; Chatterjee, A.; Janes, J.; Yan, S. F.; Trager, R.; Caldwell, J. S.; Schultz, P. G.; Zhou, Y.; Winzeler, E. A. In silico activity profiling reveals the mechanism of action of antimalarials discovered in a high-throughput screen. *Proc. Natl. Acad. Sci. U.S.A.* **2008**, *105*, 9059–9064.
- (10) Rottmann, M.; McNamara, C.; Yeung, B. K. S.; Lee, M. C. S.; Zou, B.; Russell, B.; Seitz, P.; Plouffe, D. M.; Dharia, N. V.; Tan, J.; Cohen, S. B.; Spencer, K. R.; González-Páez, G. E.; Lakshminarayana, S. B.; Goh, A.; Suwanarusk, R.; Jegla, T.; Schmitt, E. K.; Beck, H.-P.; Brun, R.; Nosten, F.; Renia, L.; Dartois, V.; Keller, T. H.; Fidock, D. A.; Winzeler, E. A.; Diagona, T. T. Spiroindolones, a Potent Compound Class for the Treatment of Malaria. *Science* **2010**, *329*, 1175–1180.
- (11) Yeung, B. K. S.; Zou, B.; Rottmann, M.; Lakshminarayana, S. B.; Ang, S. H.; Leong, S. Y.; Tan, J.; Wong, J.; Keller-Maerki, S.; Fischli, C.; Goh, A.; Schmitt, E. K.; Krastel, P.; Franco, E.; Kuhlen, K.; Plouffe, D.; Henson, K.; Wagner, T.; Winzeler, E. A.; Petersen, F.; Brun, R.; Dartois, V.; Diagona, T. T.; Keller, T. H. Spirotetrahydro β -Carbolines (Spiroindolones): A New Class of Potent and Orally Efficacious Compounds for the Treatment of Malaria. *J. Med. Chem.* **2010**, *53*, 5155–5164.
- (12) Wu, T.; Nagle, A.; Kuhlen, K.; Gagaring, K.; Borboa, R.; Francek, C.; Chen, Z.; Plouffe, D.; Goh, A.; Lakshminarayana, S. B.; Wu, J.; Ang, H. Q.; Zeng, P.; Kang, M. L.; Tan, W.; Tan, M.; Ye, N.; Lin, X.; Caldwell, C.; Ek, J.; Skolnik, S.; Liu, F.; Wang, J.; Chang, J.; Li, C.; Hollenbeck, T.; Tuntland, T.; Isbell, J.; Fischli, C.; Brun, R.; Rottmann, M.; Dartois, V.; Keller, T.; Diagona, T.; Winzeler, E.; Glynne, R.; Tully, D. C.; Chatterjee, A. K. Imidazolopyperazines: Hit to Lead Optimization of New Antimalarial Agents. *J. Med. Chem.* **2011**, *54*, 5116–5130.
- (13) Nagle, A.; Wu, T.; Kuhlen, K.; Gagaring, K.; Borboa, R.; Francek, C.; Chen, Z.; Plouffe, D.; Lin, X.; Caldwell, C.; Ek, J.; Skolnik, S.; Liu, F.; Wang, J.; Chang, J.; Li, C.; Liu, B.; Hollenbeck, T.; Tuntland, T.; Isbell, J.; Chuan, T.; Alper, P. B.; Fischli, C.; Brun, R.; Lakshminarayana, S. B.; Rottmann, M.; Diagona, T. T.; Winzeler, E. A.; Glynne, R.; Tully, D. C.; Chatterjee, A. K. Imidazolopyperazines: Lead Optimization of the Second-Generation Antimalarial Agents. *J. Med. Chem.* **2012**, *55*, 4244–4273.
- (14) Younis, Y.; Douelle, F.; Feng, T.-S.; Cabrera, D. G.; Manach, C. L.; Nchinda, A. T.; Duffy, S.; White, K. L.; Shackelford, D. M.; Morizzi, J.; Manila, J.; Katneni, K.; Bhamidipati, R.; Zabiulla, K. M.; Joseph, J. T.; Bashyam, S.; Waterson, D.; Witty, M. J.; Hardick, D.; Wittlin, S.; Avery, V.; Charman, S. A.; Chibale, K. 3,5-Diaryl-2-aminopyridines as a Novel Class of Orally Active Antimalarials Demonstrating Single Dose Cure in Mice and Clinical Candidate Potential. *J. Med. Chem.* **2012**, *55*, 3479–3487.
- (15) Younis, Y.; Douelle, F.; González Cabrera, D.; Le Manach, C.; Nchinda, A. T.; Paquet, T.; Street, L. J.; White, K. L.; Zabiulla, K. M.; Joseph, J. T.; Bashyam, S.; Waterson, D.; Witty, M. J.; Wittlin, S.; Charman, S. A.; Chibale, K. Structure–Activity–Relationship Studies around the 2-Amino Group and Pyridine Core of Antimalarial 3,5-Diarylaminopyridines Lead to a Novel Series of Pyrazine Analogues with Oral in Vivo Activity. *J. Med. Chem.* **2013**, *56*, 8860–8871.
- (16) Le Manach, C.; Nchinda, A. T.; Paquet, T.; González Cabrera, D.; Younis, Y.; Han, Z.; Bashyam, S.; Zabiulla, M.; Taylor, D.; Lawrence, N.; White, K. L.; Charman, S. A.; Waterson, D.; Witty, M. J.; Wittlin, S.; Botha, M. E.; Nondaba, S. H.; Reader, J.; Birkholtz, L.-M.; Jiménez-Díaz, M. B.; Martínez, M. S.; Ferrer, S.; Angulo-Barturen, I.; Meister, S.; Antonova-Koch, Y.; Winzeler, E. A.; Street, L. J.; Chibale, K. Identification of a Potential Antimalarial Drug Candidate from a Series of 2-Aminopyrazines by Optimization of Aqueous Solubility and Potency across the Parasite Life Cycle. *J. Med. Chem.* **2016**, *59*, 9890–9905.
- (17) Paquet, T.; Le Manach, C.; Cabrera, D. G.; Younis, Y.; Henrich, P. P.; Abraham, T. S.; Lee, M. C. S.; Basak, R.; Ghidelli-Disse, S.; Lafuente-Monasterio, M. J.; Bantscheff, M.; Ruecker, A.; Blagborough, A. M.; Zakutansky, S. E.; Zeeman, A.-M.; White, K. L.; Shackelford, D. M.; Manila, J.; Morizzi, J.; Scheurer, C.; Angulo-Barturen, I.; Martínez, M. S.; Ferrer, S.; Sanz, L. M.; Gamo, F. J.; Reader, J.; Botha, M.; Decherig, K. J.; Sauerwein, R. W.; Tungtaeng, A.; Vanachayangkul, P.; Lim, C. S.; Burrows, J.; Witty, M. J.; Marsh, K. C.; Bodenreider, C.; Rochford, R.; Solapure, S. M.; Jiménez-Díaz, M. B.; Charman, S. A.; Donini, C.; Campo, B.; Birkholtz, L.-M.; Hanson, K. K.; Drewes, G.; Kocken, C. H. M.; Delves, M. J.; Leroy, D.; Fidock, D. A.; Waterson, D.; Street, L. J.; Chibale, K. Antimalarial efficacy of MMV390048, an inhibitor of *Plasmodium* phosphatidylinositol 4-kinase. *Sci. Transl. Med.* **2017**, *9*, No. ead9735.
- (18) Ashton, T. D.; Devine, S. M.; Möhrle, J. J.; Laleu, B.; Burrows, J. N.; Charman, S. A.; Creek, D. J.; Sleeb, B. E. The Development Process for Discovery and Clinical Advancement of Modern Antimalarials. *J. Med. Chem.* **2019**, *62*, 10526–10562.
- (19) Xue, L.; Shi, D.-H.; Harjani, J. R.; Huang, F.; Beveridge, J. G.; Dingjan, T.; Ban, K.; Diab, S.; Duffy, S.; Lucantoni, L.; Fletcher, S.; Chiu, F. C. K.; Blundell, S.; Ellis, K.; Ralph, S. A.; Wirjanata, G.; Teguh, S.; Noviyanti, R.; Chavchich, M.; Creek, D.; Price, R. N.; Marfurt, J.; Charman, S. A.; Cuellar, M. E.; Strasser, J. M.; Dahlin, J. L.; Walters, M. A.; Edstein, M. D.; Avery, V. M.; Baell, J. B. 3,3'-Disubstituted 5,5'-Bi(1,2,4-triazine) Derivatives with Potent in Vitro and in Vivo Antimalarial Activity. *J. Med. Chem.* **2019**, *62*, 2485–2498.

- (20) Peters, W.; Portus, J. H.; Robinson, B. L. The chemotherapy of rodent malaria, XXII. *Ann. Trop. Med. Parasitol.* **1975**, *69*, 155–171.
- (21) Courcot, B.; Tran, D. N.; Fraisse, B.; Bonhomme, F.; Marsura, A.; Ghermani, N. E. Electronic Properties of 3,3'-Dimethyl-5,5'-bis(1,2,4-triazine): Towards Design of Supramolecular Arrangements of N-Heterocyclic CuI Complexes. *Chem. – Eur. J.* **2007**, *13*, 3414–3423.
- (22) Ban, K.; Duffy, S.; Khakham, Y.; Avery, V. M.; Hughes, A.; Montagnat, O.; Katneni, K.; Ryan, E.; Baell, J. B. 3-Alkylthio-1,2,4-triazine dimers with potent antimalarial activity. *Bioorg. Med. Chem. Lett.* **2010**, *20*, 6024–6029.
- (23) Duffy, S.; Avery, V. M. Development and Optimization of a Novel 384-Well Anti-Malarial Imaging Assay Validated for High-Throughput Screening. *Am. J. Trop. Med. Hyg.* **2012**, *86*, 84–92.
- (24) Stenberg, P.; Norinder, U.; Luthman, K.; Artursson, P. Experimental and computational screening models for the prediction of intestinal drug absorption. *J. Med. Chem.* **2001**, *44*, 1927–1937.
- (25) Sanz, L. M.; Crespo, B.; De-Cózar, C.; Ding, X. C.; Llergo, J. L.; Burrows, J. N.; Garcia-Bustos, J. F.; Gamo, F.-J. *P. falciparum* In Vitro Killing Rates Allow to Discriminate between Different Antimalarial Mode-of-Action. *PLoS One* **2012**, *7*, No. e30949.
- (26) Desjardins, R. E.; Canfield, C. J.; Haynes, J. D.; Chulay, J. D. Quantitative assessment of antimalarial activity in vitro by a semiautomated microdilution technique. *Antimicrob. Agents Chemother.* **1979**, *16*, 710–718.
- (27) Baragaña, B.; Hallyburton, I.; Lee, M. C. S.; Norcross, N. R.; Grimaldi, R.; Otto, T. D.; Proto, W. R.; Blagborough, A. M.; Meister, S.; Wirjanata, G.; Ruecker, A.; Upton, L. M.; Abraham, T. S.; Almeida, M. J.; Pradhan, A.; Porzelle, A.; Martínez, M. S.; Bolscher, J. M.; Woodland, A.; Luksch, T.; Norval, S.; Zuccotto, F.; Thomas, J.; Simeons, F.; Stojanovski, L.; Osuna-Cabello, M.; Brock, P. M.; Churcher, T. S.; Sala, K. A.; Zakutansky, S. E.; Jiménez-Díaz, M. B.; Sanz, L. M.; Riley, J.; Basak, R.; Campbell, M.; Avery, V. M.; Sauerwein, R. W.; Dechering, K. J.; Noviyanti, R.; Campo, B.; Frearson, J. A.; Angulo-Barturen, I.; Ferrer-Bazaga, S.; Gamo, F. J.; Wyatt, P. G.; Leroy, D.; Siegl, P.; Delves, M. J.; Kyle, D. E.; Wittlin, S.; Marfurt, J.; Price, R. N.; Sinden, R. E.; Winzeler, E. A.; Charman, S. A.; Bebrevska, L.; Gray, D. W.; Campbell, S.; Fairlamb, A. H.; Willis, P. A.; Rayner, J. C.; Fidock, D. A.; Read, K. D.; Gilbert, I. H. A novel multiple-stage antimalarial agent that inhibits protein synthesis. *Nature* **2015**, *522*, 315–320.
- (28) Meister, S.; Plouffe, D. M.; Kuhlen, K. L.; Bonamy, G. M.; Wu, T.; Barnes, S. W.; Bopp, S. E.; Borboa, R.; Bright, A. T.; Che, J.; Cohen, S.; Dharia, N. V.; Gagaring, K.; Gettayacamin, M.; Gordon, P.; Groessl, T.; Kato, N.; Lee, M. C.; McNamara, C. W.; Fidock, D. A.; Nagle, A.; Nam, T. G.; Richmond, W.; Roland, J.; Rottmann, M.; Zhou, B.; Froissard, P.; Glynn, R. J.; Mazier, D.; Sattabongkot, J.; Schultz, P. G.; Tuntland, T.; Walker, J. R.; Zhou, Y.; Chatterjee, A.; Diagana, T. T.; Winzeler, E. A. Imaging of Plasmodium liver stages to drive next-generation antimalarial drug discovery. *Science* **2011**, *334*, 1372–1377.
- (29) Stickles, A. M.; de Almeida, M. J.; Morrissey, J. M.; Sheridan, K. A.; Forquer, I. P.; Nilsen, A.; Winter, R. W.; Burrows, J. N.; Fidock, D. A.; Vaidya, A. B.; Riscoe, M. K. Subtle changes in endochin-like quinolone structure alter the site of inhibition within the cytochrome bc1 complex of *Plasmodium falciparum*. *Antimicrob. Agents Chemother.* **2015**, *59*, 1977–1982.
- (30) Delves, M. J.; Miguel-Blanco, C.; Matthews, H.; Molina, I.; Ruecker, A.; Yahiya, S.; Straschil, U.; Abraham, M.; Leon, M. L.; Fischer, O. J.; Rueda-Zubiaurre, Brandt, J. R.; Cortes, A.; Barnard, A.; Fuchter, M. J.; Calderon, F.; Winzeler, E. A.; Sinden, R. E.; Herreros, E.; Gamo, F. J.; Baum, J. A high throughput screen for next-generation leads targeting malaria parasite transmission. *Nat. Commun.* **2018**, *9*, No. 3805.
- (31) Wadi, I.; Nath, M.; Anvikar, A. R.; Singh, P.; Sinha, A. Recent advances in transmission-blocking drugs for malaria elimination. *Future Med. Chem.* **2019**, *11*, 3047–3089.
- (32) Vaughan, A. M.; Kappe, S. H. I.; Ploss, A.; Mikolajczak, S. A. Development of humanized mouse models to study human malaria parasite infection. *Future Microbiol.* **2012**, *7*, 657.
- (33) Jiménez-Díaz, M. B.; Mulet, T.; Gómez, V.; Viera, S.; Alvarez, A.; Garuti, H.; Vázquez, Y.; Fernández, A.; Ibáñez, J.; Jiménez, M.; Gargallo-Viola, D.; Angulo-Barturen, I. Quantitative measurement of Plasmodium-infected erythrocytes in murine models of malaria by flow cytometry using bidimensional assessment of SYTO-16 fluorescence. *Cytometry, Part A* **2009**, *75A*, 225–235.
- (34) Baell, J. B.; Holloway, G. A. New Substructure Filters for Removal of Pan Assay Interference Compounds (PAINS) from Screening Libraries and for Their Exclusion in Bioassays. *J. Med. Chem.* **2010**, *53*, 2719–2740.
- (35) Saubern, S.; Guha, R.; Baell, J. B. KNIME Workflow to Assess PAINS Filters in SMARTS Format. Comparison of RDKit and Indigo Cheminformatics Libraries. *Mol. Inf.* **2011**, *30*, 847–850.